# Dynamical Climatology

## A comparison of the impact of an envelope orography and of a parametrization of orographic gravity-wave drag on model simulations.

by

A. Slingo and D.W. Pearson

DCTN 43

June 1986

Meteorological Office (Met. O. 20)
London Road
Bracknell
Berkshire RG12 2SZ

DYNAMICAL CLIMATOLOGY TECHNICAL NOTE NO. 43

# A COMPARISON OF THE IMPACT OF AN ENVELOPE OROGRAPHY AND OF A PARAMETRIZATION OF OROGRAPHIC GRAVITY-WAVE DRAG ON MODEL SIMULATIONS

by

A Slingo and D W Pearson

Submitted for publication in Quart. J. R. Met. Soc.

Met O 20 (Dynamical
Climatology Branch)
Meteorological Office
London Road
Bracknell
Berkshire, U.K. RG12 2SZ

Note: This paper has not been published. Permission to quote from it should be obtained from the Assistant Director of the above Meteorological Office branch.

# A COMPARISON OF THE IMPACT OF AN ENVELOPE OROGRAPHY AND OF A PARAMETRIZATION OF OROGRAPHIC GRAVITY-WAVE DRAG ON MODEL SIMULATIONS

by

A. Slingo* and D.W. Pearson

Meteorological Office, Bracknell

Submitted to Quart. J. R. Met. Soc.

June 1986

* This paper was completed while on leave at the National Center for Atmospheric Research, Boulder, Colorado 80307, USA. The National Center for Atmospheric Research is sponsored by the National Science Foundation.

## SUMMARY

Results are presented from extended annual-cycle integrations of the Meteorological Office 11-Layer Atmospheric General Circulation Model. An 8 year control integration produces a good simulation in the southern hemisphere in both summer and winter and also in the northern hemisphere in summer. In northern winter, however, there is excessive westerly near-surface flow polewards of about $40^0$ N. It is argued that this indicates a lack of orographic forcing of the flow by the major mountain ranges. Two solutions which have been proposed for this problem are investigated. The first is envelope orography and the second is a parametrization of the effects of orographic gravity wave drag. Each was included separately in 3 1/2 year integrations in parallel with the control. Both produce substantial changes in the model's climatology, but envelope orography does not improve the westerly problem over the European area and it also degrades the summer circulation. The gravity wave drag scheme, however, gives results which in general are in very good agreement with the observations in both hemispheres and seasons. A study of the variability of the 500 mb height fields on synoptic timescales demonstrates the improvement in the positions of the northern hemisphere storm tracks in this integration. Some remaining errors in the simulations are identified, particularly in the stratosphere. Finally, it is argued that despite these results it may be too early to come to a final conclusion as to the role of gravity wave drag in the general circulation and also as to the relative importance of dynamical and radiative processes in the polar winter stratosphere.

# 1. INTRODUCTION

It has long been recognized that Atmospheric General Circulation Models (AGCMs) should be integrated at as high a resolution as computing resources will allow, in order to resolve important features of the general circulation such as baroclinic wave development, to facilitate investigations of regional aspects of the circulation and of climate sensitivity , and to minimise the effects of numerical approximations (e.g Manabe et al. 1970). As the resolution is increased, one would hope that the realism of the simulations would also improve. In many respects this has been shown to be the case, especially in the field of numerical weather prediction where the horizontal resolution used in global models has been increased progressively over the past two decades towards $1^0$ (Gadd 1985; ECMWF 1985). It is also generally true for AGCMs integrated for longer periods to provide climate simulations. For example, precipitation patterns become better defined and the circumpolar trough in the southern hemisphere becomes deeper and thus more realistic. However, in the mid-latitudes of the northern hemisphere in winter the westerly flow tends to become too strong at the surface, in association with excessively deep low pressure areas over the north Atlantic and Pacific oceans (e.g. Manabe et al. 1979, Figure 2). Such behaviour is common to both grid- point and spectral models and leads to poor simulations of the northern hemisphere winter near-surface flow for models with a horizontal resolution finer than about $4^0$ of latitude. This westerly problem is generally absent in low resolution models, which are of course computationally fast so that integrations through many annual cycles are possible. Spectral models with rhomboidal truncation at 15 waves have been quite successful in simulating the northern hemisphere winter flow (Manabe and Hahn 1981; Pitcher et al. 1983). However, the spectral model with similar resolution (triangular truncation at 20 waves) described by Boer et al. (1984a,b) suffers from a westerly problem unless a parametrization of gravity wave drag is included (McFarlane 1986).

A particularly well developed example of the westerly problem is shown in Figure 1, in which the distribution of pressure at mean sea level (PMSL) for the northern winter season from a multi-annual cycle integration of the Meteorological Office 11-Layer AGCM is compared with the observed distribution. Details of the model are given in the next section.

In the southern hemisphere the strengths and position of the sub-tropical high pressure cells and of the circumpolar depression belt are well simulated. In the northern hemisphere, however, there is excessive westerly flow over the mid-latitudes. This is associated with pressures which are far too low at high latitudes, the north Atlantic low pressure area being about 20mb too deep and displaced north- eastwards from its climatological position. The strong westerly flow over Europe is exacerbated by an over-intense sub-tropical high pressure cell which is positioned just west of the Greenwich meridian.

The observed PMSL distributions for northern winter (Figure 1a) and northern summer (Figure 2a) show considerable differences between the two hemispheres. In the southern hemisphere there is strong mid-latitude flow which in the mean is predominantly westerly with little longitudinal variation and little change from one season to the other. In contrast, in the northern hemisphere the substantial land area and the presence of several major mountain ranges produce a weaker mean flow with considerable variations in the meridional component. In winter there are high pressure cells over the continents and low pressure over the oceans, whereas in summer this is reversed with extensive heat lows over the land. The asymmetric land-sea distribution is clearly the cause of the differences between the hemispheres, but the precise reasons have been debated for many years (e.g. Hoskins and Karoly 1981). Two factors which have received the most attention are orographic forcing of the flow by the major mountain ranges and thermal forcing brought about by the different thermal characteristics of land and sea. Other differences include the surface roughness which is generally higher over land and shows large geographical variations, while over the sea it is dependent on the wind speed (Garratt 1977; Wu 1982).

In contrast with the northern winter season, the PMSL pattern is well simulated by the model in the northern summer (Figure 2). In the northern hemisphere the heat lows and oceanic highs are in their correct locations and with central values close to the observed, although pressures are a few millibars too low over the southern part of North America. The spurious trough extending from the Asian heat low into the western Pacific is associated with an over-intense area of precipitation. The southern hemisphere pattern is again in good agreement with the observations.

The fact that the westerly problem arises only in the northern winter, when the flow is strongest, and the similarity of the modelled flow to that in the southern hemisphere, strongly suggests that the dynamical forcing by the land- sea distribution is too weak in this season. Efforts to remove this error have thus concentrated on increasing the magnitude of the forcing. In particular , two solutions have been proposed which increase the magnitude of the orographic component, although in radically different ways.

Wallace et al. (1983) demonstrated that the systematic errors in the ECMWF forecast model could be reduced by enhancing the land surface elevations preferentially over the major mountain ranges. The elevations were increased by adding to the usual grid-box averaged value an increment proportional to the standard deviation of the sub-gridscale variation, derived from a high resolution dataset. It was argued that such an "envelope orography" represents the blocking effect of the highest peaks and ridges in a mountain range, so that the response of the large-scale flow is determined by the envelope defined by these features rather than by the mean elevation. One notable advantage of this idea is its simplicity and ease of application, especially when sigma-coordinates are used as the only modification then required is to change the dataset specifying the geopotential height of the lower boundary.

A very different approach has been followed by Palmer et al.(1986). They presented evidence to show that the atmospheric drag induced by breaking gravity waves excited by flow over mountain ranges is an important term in the global momentum budget. By ignoring this process most AGCMs underestimate the effective surface drag. This underestimate can then lead to a compensating increase in the mean westerly winds. They developed a parametrization of the effects of gravity-wave drag for the 11-Layer Model and obtained substantial improvements in the climatology of a version integrated for perpetual January conditions.

Several projects in progress at the Meteorological Office require the 11-Layer AGCM to be integrated with seasonally-varying forcing through many annual cycles. Any solution to the westerly problem in this model must therefore not only produce good simulations in northern winter, but must also not degrade what is already realistic behaviour in summer. The purpose of this study was therefore to compare the effects of an envelope orography and

of the gravity wave scheme in extended integrations lasting several years, with emphasis on the mean fields and their variations on synoptic timescales. This work is an extension of the pilot study reported by Slingo and Wilson (1986). Results from a control integration and from integrations with envelope orography and the gravity wave scheme are here compared with each other and with observations. No attempt is made to provide detailed explanations of the differences between the simulations, as this is the subject of a separate study (Palmer et al., in preparation).

## 2. SUMMARY OF MODEL AND EXPERIMENTS

The 11-Layer Model is a global finite-difference AGCM with a regular latitude-longitude grid, which is integrated on a Cyber 205 computer. The version employed has a horizontal resolution of 2.5 x 3.75 degrees and is the same as that used by Palmer and Mansfield (1986) and Palmer et al. (1986), apart from minor differences. Table 1 lists a brief specification of the version used for the control simulation. At each grid point, the two horizontal components of wind,the temperature and the humidity mixing ratio (u,v,T,q) are held at 11 levels whose sigma values (pressure divided by the surface value $p_*$ ) are 0.98744, 0.93701, 0.84380, 0.71772, 0.57717, 0.43626, 0.31738, 0.23047, 0.15741, 0.08856 and 0.02207. The model was integrated with seasonally-varying forcing and the prescribed sea surface temperatures, sea-ice limits, ozone and cloud amounts were updated in a similar way to previous integrations of the 5-Layer Model (J.M. Slingo 1982). A cloud prediction scheme has since been included in the model, but was not completed when this work was performed. A detailed description of the model is available (Slingo 1985b).

The experiments studied here all use initial data taken from the end of August from the fifth year of an existing annual-cycle integration. The control experiment (often referred to within the Meteorological Office as the Third Annual-Cycle Control Integration) was continued for a further 8 years and the envelope orography and gravity wave integrations for a further 3 1/2 years. For the control and gravity wave experiments the land surface elevations in each grid box were taken as the mean of the values in a $1^0$ x $1^0$ dataset (Gates and Nelson 1973). The envelope orography was created by adding to these elevations an increment equal to twice the standard deviation of the values within each grid box,calculated from the U.S. Navy high resolution (one-sixth of a degree) dataset, which was also employed by Wallace et al. (1983). In early experiments with such an orography the large increments added in some areas (notably over the Andes) led to spurious oscillations in the modelled geopotential height fields. The problem was overcome by limiting the value of the increment to a maximum of 1500m. This truncation of the envelope orography took place over only a small number of grid points and was very effective in controlling

the oscillations. The version of the gravity wave scheme used is that described by Palmer et al. (1986).

Mean fields from the model integrations are compared with observed data derived from Meteorological Office operational analyses in Figures 1-14. The maps are global with latitudes and longitudes drawn every $30^0$ and with the model's land-sea mask as background. In all the maps the data have been interpolated to a $5^0$ x $5^0$ grid for clarity at this scale of reproduction. The observed data are averages over three northern winters (1983/4 to 1985/6) and three summers (1983-5). While this is too short a period to provide a reliable climatology, the data are believed to be of high quality and in general the fields shown here agree very well with published climatologies (e.g. see Boer et al. (1984b) and Oort (1983). One difference is worth noting, however. The zonal-mean temperature at the tropical tropopause is 198 K in Figure 5a (December to February) and 201 K in Figure 6a (June to August). These temperatures agree with ECMWF analyses for a similar period (e.g. Arpe and Klinker 1986), but are about 5 K warmer than the values obtained by a direct analysis of radiosonde data for 1958 to 1973 (Oort 1983).

The results from the control simulation are discussed in the next section and those from the truncated envelope orography and gravity wave drag integrations are compared in section 4. The ability of each version of the model to reproduce the observed patterns of variability on synoptic timescales is assessed in section 5.

## 3. CONTROL SIMULATION

As discussed in the introduction, in the northern winter the control integration produces a good simulation of the PMSL distribution in the southern hemisphere, with a deep circumpolar trough positioned close to the edge of Antarctica (Figure 1). The sub-tropical high pressure cells are also located correctly, although they are about 3 mb too intense. In the northern hemisphere the pressure at high latitudes is far too low, by over 20 mb in places, so that there is excessive westerly near-surface flow at about $60^0N$. The Icelandic low is also much too far to the east. The strong sub-tropical high pressure area centred over the Greenwich meridian is an interesting feature as it can also be seen in several other AGCM results. It tends to intensify together with the westerly problem as the resolution is increased (Manabe et al. 1979), but may also be present when the flow is otherwise quite realistic (e.g. Boer et al. 1984b; Randall et al. 1985). The existence of this high is reflected in the 500mb height field (Figure 3) as an area of exaggerated diffluence. Apart from this feature the standing wave pattern in the northern hemisphere is fairly realistic in middle latitudes. In the tropics the heights are a few decametres lower than the observed values, indicating that the lower troposphere is slightly too cold. A much larger difference is evident at high northern latitudes, with a height deficit in excess of 20 decametres over the north pole. The meridional gradient in the height field is thus much too strong, so that the westerly bias in the surface winds shown by the PMSL field is also present at this level. This bias may also be seen in the 250 mb wind field (Figure 4), especially over central Asia where the flow appears as a continuation of the North Atlantic jet. In reality this jet decelerates before landfall (Figure 4a), but in the control integration it is extended too far in the zonal direction. This suggests that disturbances in the storm track are propagating too far eastwards before decaying, which is consistent with the surface pressure field and is confirmed by the data to be presented in section 5. In contrast, the acceleration into the entrance of the sub-tropical jet over North Africa is simulated reasonably well, although by the time the jet reaches the Pacific the wind speeds are too low by roughly $10ms^{-1}$. In the southern hemisphere the latitude (about $50^0$ S) and maximum wind speed (just under $40ms^{-1}$) of the jet are in good agreement with the observations.

Comparison of the zonally-meaned winds and temperatures for northern winter (Figure 5) and summer (Figure 6) reveals some important features. In the northern hemisphere in winter the magnitude of the westerly wind error increases with height to the north of $40^0$ N , so that there is an excessively strong polar night jet and temperatures about 20K too cold over the pole at the highest level. The maximum of the tropospheric sub-tropical jet is at about the correct pressure and latitude, although weaker than the observed. There is also a spurious secondary maximum at about $50^0$ N. The resulting double structure in the troposphere is very similar to that in both the modelled and (to a lesser degree ) the observed data for the southern hemisphere in the southern winter (Figure 6).

These figures show additional errors which are not directly related to the westerly problem in the northern hemisphere in winter. In this season (Figure 5), the observations in the southern hemisphere show a jet maximum at about 250 mb and the winds become easterly by about 50 mb. In the model the jet maximum is at about 150 mb and there are mean westerly winds of $29ms^{-1}$ even at the top model level (about 22 mb) at this latitude. In association with these wind errors the observed reversal of the sign of the latitudinal temperature gradient above about 200 mb is too weak. The stratosphere is thus poorly represented in the southern hemisphere although the tropospheric simulation is good. This combination seems in conflict with the conclusion of Boville (1984) that inaccuracies in the stratospheric simulation of an AGCM will produce errors in the tropospheric simulation, but his results were obtained for the northern hemisphere in winter, where the quasi-stationary planetary waves are much stronger. In northern summer (Figure 6), the northern hemisphere jet is also too high in the model, is slightly too strong and the stratospheric winds too westerly. The stratospheric temperatures increase rapidly with height whereas they should be close to isothermal. Both these errors are of the same character as those shown in the southern hemisphere in Figure 5b. In the southern hemisphere winter, Figure 6b shows a stratospheric polar night jet at least $10ms^{-1}$ too strong and polar temperatures up to about 10K too low. Again, similar errors were found in the northern hemisphere in winter. A significant component of the stratospheric wind and temperature errors thus cannot be due to errors in the orographic forcing, because they show strong symmetry between the two hemispheres in each season. Errors in representing

the effects of orography should be much smaller in the southern hemisphere and in the northern hemisphere in summer, compared with the northern hemisphere winter. Possible causes of these errors are insufficient vertical resolution and an inadequate treatment of radiative processes. Work is planned to investigate each of these areas.

The final diagnostic from the control integration is the distribution of total precipitation (rain plus snow) for northern winter, which is compared with Jaeger's climatology (1983) in Figure 7. At low latitudes the pattern is well represented by the model, with maxima over south America, southern Africa and Indonesia and in the ITCZ. There are minima in the correct locations over the sub-tropics, although these dry zones do not extend sufficiently far to the west over the oceans. This deficiency has since been rectified by various changes to the model which were necessary to improve the cloudiness simulation (Slingo et al. 1986, in preparation). In the extra-tropics the pattern is also good with maxima in the depression belts over the southern ocean and north Atlantic and Pacific oceans, although peak amounts differ from those in Jaeger's data. Evidence of the westerly problem may be seen in the northern hemisphere ; the 1 mm/day contour extends too far to the east over both north America and northern Asia.

Leaving aside the question of the stratospheric simulation, many of the errors identified earlier for the northern hemisphere winter are consistent, at least qualitatively, with the hypothesis of insufficient forcing of the flow by the major mountain ranges. Too little forcing (because of insufficient mountain torque, surface stress or gravity wave stress) would be expected to lead to an acceleration of the flow, which would become too zonally symmetric. The reduced convergence of heat into the high latitudes would lead to a cooling of the polar atmosphere until a new balance was established with the longwave radiative cooling and the surface turbulent fluxes. This argument was the rationale behind carrying out the experiments with the truncated envelope orography and gravity wave drag scheme.

## 4. SIMULATIONS WITH ENVELOPE OROGRAPHY AND GRAVITY WAVE DRAG

In this and the following sections, the truncated envelope orography experiment will be referred to as TENV and the experiment with the gravity wave drag scheme as GRAV. In both cases there are substantial improvements in the PMSL distribution in the northern hemisphere in winter, while the southern hemisphere results are essentially unchanged (Figure 8). In GRAV the Icelandic low is now in its correct location (although the central pressure is still slightly too low) and the high pressure area to the south has weakened. The near-surface flow over western Europe is thus weaker and more south-westerly than in the control experiment, in good agreement with the observations. In TENV, however, the low pressure area is in the same position as in the control (although less deep) and the high has moved further north. In both experiments the high pressure cells over northern Asia and America are much better represented. The Aleutian low is still too deep in GRAV and in this area the results from TENV are closer to the observed pressures.

The effects of GRAV outlined above are similar to those found by Palmer et al. (1986), although the improvement over the European area is more dramatic. It is not clear whether the differences are significant, however, as their results were taken from the mean of only 60 days of model simulation.

In both integrations the 500 mb heights (Figure 9) are increased by about 10 dam at high northern latitudes compared with the control (Figure 3). This is an improvement, although only about half the original underestimate has been removed. The standing wave pattern has also been enhanced, especially in TENV where the two low centres over northern Canada and eastern Siberia are well represented. However, the poleward shift of the contours in the north Atlantic ridge, associated with the movement of the sub-tropical anticyclone, is unrealistic. In both TENV and GRAV the reduction in the zonally-meaned equator to north pole height gradient means that the westerly problem has been reduced at this level, although the enhanced gradient over the west Pacific indicates an acceleration of the jet. At 250 mb (Figure 10) the velocities at the cores of the Atlantic/Pacific jets from TENV ($44/71 ms^{-1}$) and GRAV ($46/73 ms^{-1}$) are also higher than in the control ($40/64 ms^{-1}$) and are closer to the observed values ($44/76 ms^{-1}$). In TENV the Atlantic

jet is oriented too far to the north, as would be expected from the previous figures. This jet is quite realistic in GRAV, but even here the tendency for insufficient deceleration at the jet exit is still to be seen.

The zonally-meaned winds (Figure 11) confirm the acceleration of the northern hemisphere sub-tropical jet and the reduction in the westerly problem to the north. The stratospheric polar-night jet is decelerated and in conjunction with this there are temperature rises over the pole of up to about 20 K. These effects are more pronounced in GRAV than in TENV. As would be expected, the southern hemisphere simulation is little different from the control in either integration. The northern hemisphere simulation in GRAV is in good agreement with the observed (Figure 5a) , except that the stratospheric winds above the sub-tropical jet now show the same westerly bias as was noted for the control integration in the northern hemisphere in summer (Figure 6) and in the southern hemisphere in either season (Figures 5 and 6).

For both TENV and GRAV the reduction in the westerly problem leads to small improvements in the precipitation distributions (Figure 12) compared with the control (Figure 7b). Over most of north America and northern Eurasia the precipitation rates are reduced. Note, for example, that the 1 mm/day contour is further south both over north America and also at about $75^0E$. There are increases in the precipitation rates over the north Atlantic and Pacific oceans. These changes suggest that there are improvements in the positions of the northern hemisphere storm tracks. This interpretation is consistent with the results to be shown in the next section. In the tropics and in the southern hemisphere the differences from the control simulation are small and are not significant.

It was shown in the previous section that the control integration produces a realistic PMSL distribution in the northern summer (Figure 2). This field thus provides a test of whether envelope orography and the gravity wave drag scheme are applicable in summer as well as winter and hence whether they are suitable for inclusion in seasonally-varying integrations. The results from GRAV (Figure 13b) are very close to those from the control, indicating that the stability-dependence incorporated into the parametrization has effectively 'turned off' the scheme. On the other hand, the intensities of the northern hemisphere continental lows and oceanic highs are exaggerated in TENV (Figure 13a) and

the pressure is also too high over the pole. It would appear that in this season the land surface elevations are too high, so that the thermal forcing of the continental heat lows is too pronounced, leading to a compensating increase in pressure over the oceans.

The zonally-averaged winds and temperatures in the northern summer from TENV and GRAV (Figure 14) are very similar to the control. In GRAV there is a small improvement in the latitude of the northern hemisphere jet and in the stratospheric winds. Otherwise, the systematic errors noted earlier in the stratosphere are still evident.

The statistical significance of the differences between the results from these integrations and the control was assessed by calculating t-statistics. For 10 degrees of freedom (8 winters from the control plus 4 winters from each experiment minus 2) t will on average exceed $\pm 3.17$ only 1 per cent of the time if the means tested are from the same population. The major changes noted in this section have t values in excess of this over large areas and hence are highly significant, as one would expect from the magnitude of the changes.

## 5. VARIABILITY ON SYNOPTIC TIMESCALES

Variability is an important property of the atmospheric general circulation, so that for a model of this system to be realistic it must be able to reproduce not only the observed mean state but also the fluctuations over various time-scales. The analysis in this section concentrates on the variations on the synoptic time-scale for the northern winter season.

The technique of filtering daily or twice-daily sampled fields was developed by Blackmon (1976) and others in order to separate the contributions to atmospheric variability from synoptic features (time-scales less than one week) and from lower frequency changes (e.g. associated with blocking). Filtering has been used in studies of the real atmosphere and also in the analysis of AGCM integrations (e.g. Malone et al. 1984). High-pass filtering reveals elongated maxima over the north Atlantic and Pacific oceans which are due to synoptic features propagating along the so-called 'storm tracks'. In this section, such a filter is applied to daily 500 mb height fields from both the model and from the Meteorological Office analyses.

The high pass variance was calculated from the difference between the variance of the daily fields and the variance of 3-day mean fields. This is designed to select fluctuations with a period of up to about 6 days. The variances were calculated separately for each year and the results shown here were obtained by averaging over all the years in each case ( i.e. over 3 samples for the observed data, 8 for the control and 4 for both TENV and GRAV).

Figure 15a shows the results for the Meteorological Office analyses. The storm tracks over the north Atlantic and Pacific oceans are clearly visible , as is a minor maximum over northern Asia at about $75^0$ E. There is a minimum over the north pole and the variability also drops rapidly towards the equator. The pattern is very similar to that shown in Figure 15 of Malone et al. (1984), who used data from an earlier period, although the values in the storm tracks are about 20 per cent larger. It is not clear whether this disagreement is due to real differences between the different periods or to the fact that Malone et al. (1984) calculated their variances in a different way to that used here.

In the control integration (Figure 15b) both storm tracks are poorly represented and are displaced north-eastwards. The maximum in the Pacific storm track is thus over western Canada whereas it should be near the dateline and that in the Atlantic is over Iceland whereas it should be over Newfoundland. The data thus indicate that disturbances are propagating too far east over the continents, which is consistent with the errors in the surface pressure distribution shown in Figure 1b. It should also be noted that there is an underestimate of the standard deviation at low latitudes, as shown for example by the latitude of the 1 dam contour.

In experiment TENV the standard deviation is generally lower than in both the control and the observations and the positions of the storm tracks are still poor (Figure 15c). There is little change in the position of the Atlantic storm track, which is consistent with the fact that in this region the PMSL distribution (Figure 8a) is little better than in the control (Figure 1b). However, the Pacific storm track is also little different from that in the control, despite the fact that the PMSL pattern here is much improved.

The simulation of the standard deviation pattern in GRAV (Figure 15d) is much better than in either TENV or the control and is in very good agreement with the observations. However, the values are significantly lower, not only at low latitudes as noted earlier but also within the storm tracks, especially over the Atlantic ocean.

These results demonstrate the usefulness of time-filtering to isolate errors in the treatment of synoptic variability. They confirm that the simulation is generally much more realistic in experiment GRAV than in either TENV or the control. However, they give no indication as to whether that improvement is a result of a better representation of the transient features themselves, or whether it is due to an improved stationary wave pattern. That question is beyond the scope of the present study but will be addressed in a subsequent paper (Palmer et al., in preparation).

## 6. DISCUSSION

The primary motivation for this study was to find a physically acceptable solution to the westerly problem near the surface in the 11-Layer AGCM, because many of the projects for which the model is being used are concerned with impacts on the surface climate ( e.g. determining the effect of increasing carbon dioxide concentrations and of changes in land surface use). In the control experiment, the westerly problem was especially serious over Europe , the climate in winter being excessively mild, with few periods of easterly winds associated with blocking anticyclones. In summer, however, the simulation was very good . The truncated envelope orography produced results which were as good as those with the gravity wave drag scheme in many areas, but with two important exceptions. The PMSL patterns (and hence the low level winds) were worse over much of the northern hemisphere in summer and also over the European area in winter. In contrast, the gravity wave drag scheme not only eliminated the westerly problem but also preserved the good simulation in northern summer. The improvements in the geographical distribution of the variables studied is certainly impressive . This suggests that the scheme is physically reasonable, but before a firm conclusion can be reached it would be interesting to see if these improvements are maintained when other processes which affect the distribution of the surface drag are included ( e.g. variable land surface roughness and wind speed dependent exchange coefficients over the sea). In addition, the fact that so much of the drag is deposited above 200 mb (e.g. Palmer et al. 1986 , Figure 19) is of concern. It is possible that the motions induced by this drag are being distorted by the lack of sufficient vertical resolution in the model stratosphere. It was also suggested in section 3 that the high degree of symmetry between hemispheres and seasons in the wind and temperature errors may also point to lack of vertical resolution as a contributor to the errors at stratospheric levels. It would thus be of interest to repeat these experiments in a model with a much higher vertical resolution in this region. The integration with the gravity wave drag scheme is also being extended to provide improved statistics on the inter-annual variability of this version of the model.

In many basic respects the mean fields for northern winter from the integrations with the truncated envelope orography and gravity wave drag scheme show similar differences from the control. The forcing mechanism is of course very different in each case. With envelope orography the height fields (e.g. Figure 9a) are consistent with the hypothesis that increasing the orography has simply enhanced the influence of the mountains on the stationary waves. With the gravity wave scheme an additional drag is included, mainly at high levels. The effects are similar, however; an increased convergence towards the pole, with subsidence leading to a warmer atmosphere and higher surface pressures.

In both experiments TENV and GRAV the stratospheric simulations improve compared with the control, especially in the northern winter where the polar night jet is decelerated and the 'cold pole' problem removed. Given the model's lack of vertical resolution in this region, however , it would be unwise to draw general conclusions regarding the importance of orographically-induced circulations, although McFarlane (1986) found similar improvements when gravity wave drag was included in the Canadian Climate Centre model, which has higher stratospheric resolution than the 11-Layer Model. The mean state of the northern winter stratosphere is certainly determined by a balance between dynamical and radiative processes, although the relative importance of each has been a matter for much debate ( e.g. see the papers by Geller and by Mahlman and Umscheid in Holton and Matsuno (1984)). In both the present experiments and those of McFarlane, realistic simulations were produced by the inclusion of gravity wave drag. In contrast, Ramanathan et al. (1983) improved the climatology of the NCAR Community Climate Model through refinements in the treatment of radiative processes alone. One of these refinements which one would expect to be especially relevant in the stratosphere, namely the inclusion of the temperature dependence of the carbon dioxide 15 micron bands, was incorporated in the series of changes made by Slingo and Wilderspin (1986) to the 11-Layer Model, which were included in the present integrations. Separate experiments have shown that while these changes did warm the stratosphere by up to about 10 K, the effect on the polar night jet was small as the poleward temperature gradient was changed only slightly. The fact that the tropospheric westerly problem increases with the horizontal resolution of a model and that both the Canadian and Meteorological Office models respond positively

at all levels to gravity wave drag may be relevant to this debate. It suggests that for a model to provide reliable guidance as to the relative roles of dynamical and radiative processes, it should not only include an accurate radiation scheme but also have sufficient vertical resolution to resolve both the stratosphere and troposphere adequately ( say at least 10 levels in each) and at least the same horizontal resolution as the model used here. It should also, of course, produce a realistic summer and winter climatology throughout the atmosphere.

While the deficiencies in the results from experiment TENV were sufficiently serious to warrant rejection of envelope orography as a solution to the westerly problem in the 11-Layer model, the question as to what is the best recipe for constructing an orographic dataset for an AGCM remains open. It is quite conceivable that a more carefully constructed envelope orography would yield better results than that employed here. However, such an orography does not seem to be a reasonable one to use when calculating the terms in the surface heat balance, for which the 'mean' elevation is more appropriate. Apart from this, there is little evidence to suggest that a 'mean' orography has anything special to recommend it, except in terms of simplicity or in the case of a model with such a high horizontal resolution that the major effects of mountains on the flow would be resolved. For the present the gravity wave drag scheme seems the most effective solution to the westerly problem and has therefore been incorporated into a new version of the 11-Layer Model.

## ACKNOWLEDGEMENTS

The truncated envelope orography dataset was produced by Howard Wilson and the mean observed datasets derived from the Meteorological Office operational analyses were created with help from Brian Barwell. The program to calculate and display the time-filtered fields presented in section 5 was made available by Richard Swinbank. We are also grateful to John Mitchell , Peter Rowntree, Byron Boville and V. Ramanathan for their comments on the manuscript.

## REFERENCES


Arpe K. and Klinker E., 1986 : Systematic errors of the ECMWF operational forecasting model in mid-latitudes. *Quart. J. R. Met. Soc.* , **112** , 181-202.

Blackmon M. L., 1976 : A climatological spectral study of the 500 mb geopotential height of the northern hemisphere. *J. Atmos. Sci.* , **33** , 1607-1623.

Boer G. J., McFarlane N. A., Laprise R., Henderson J. D. and Blanchet J.-P., 1984a : The Canadian Climate Centre Spectral Atmospheric General Circulation Model. *Atmosphere-Ocean* , **22** , 397-429.

Boer G. J., Mcfarlane N. A. and Laprise R., 1984b : The climatology of the Canadian Climate Center General Circulation Model as obtained from a five-year simulation. *Atmosphere-Ocean* , **22** , 430-473.

Boville B. A., 1984 : The influence of the polar night jet on the tropospheric simulation in a GCM. *J. Atmos. Sci* , **41** , 1132-1142.

Carson D. J., 1982a : Current parametrizations of land-surface processes in atmospheric general circulation models. Land surface processes in atmospheric general circulation models. Ed. P. S. Eagleson. Cambridge University Press.

Carson D. J., 1982b : Comments on the sensitivity of numerical simulations to different parametrizations of the boundary-layer properties and processes. Proceedings of the Workshop on Planetary Boundary Layer Parametrization, 25-27 November 1981, ECMWF.

Corby G.A., Gilchrist A. and Rowntree P. R., 1977 : United Kingdom Meteorological Office Five-Level General Circulation Model. *Methods in Computational Physics* , **17** , 67-110.

ECMWF, 1985 : Annual Report 1984. European Centre for Medium Range Weather Forecasts, Shinfield Park, Reading, Berkshire RG2 9AX, England.

Gadd A. J., 1985 : The 15-level weather prediction model. *Meteorol. Mag.* , **114** , 222-226.

Garratt J. R., 1977 : Review of drag coefficients over oceans and continents. *Mon. Wea. Rev.* , **105** , 915-929.

Gates W. L. and Nelson A. B., 1973 : A new tabulation of the Scripps topography on a $1^0$ global grid. Part 1: Terrain Heights. R-1276-ARPA, Rand Corporation, Santa Monica, California, USA.

Holton J. R. and Matsuno T., 1984 : Dynamics of the Middle Atmosphere. Terra Scientific Publishing Company, Tokyo, Japan.

Hoskins B. J. and Karoly D. J., 1981 : The steady linear response of a spherical atmosphere to thermal and orographic forcing. *J. Atmos. Sci.* , **38** , 1179-1196.

Jaeger L., 1983 : Monthly and areal patterns of mean global precipitation. Variations in the global water budget. D. Reidel Publishing Company.

McFarlane N. A., 1986 : The effect of orographically excited gravity wave drag on the general circulation of the lower stratosphere and troposphere. To be submitted for publication.

Malone R. C., Pitcher E. J., Blackmon M. L., Puri K. and Bourke W., 1984 : The simulation of stationary and transient geopotential-height eddies in January and July with a spectral general circulation model. *J. Atmos. Sci.* , **41** , 1394-1419.

Manabe S., Hahn D. G. and Holloway J. L., 1979 : Climate simulations with GFDL spectral models of the atmosphere: Effect of spectral truncation. Report of the JOC Study Conference on Climate Models: Performance, Inter-Comparison and Sensitivity Studies. GARP Publications Series No. 22, WMO/ICSU.

Manabe S. and Hahn D.G., 1981 : Simulation of atmospheric variability. *Mon. Wea. Rev.* , **109** , 2260-2286.

Manabe S., Holloway J. L. and Stone H. M., 1970 : Simulated climatology of a general circulation model with a hydrologic cycle, III. Effects of increased horizontal computational resolution. *Mon. Wea. Rev.* , **98** , 175-212.

Oort A. H., 1983 : Global Atmospheric Circulation Statistics, 1958-1973. NOAA Professional Paper no. 14. U. S. Government Printing Office, Washington D. C. .

Palmer T. N. and Mansfield D. A., 1986 : A study of wintertime circulation anomalies during past El Nino events, using a high resolution general circulation model. I. Influence of model climatology. *Quart. J. R. Met. Soc.* , **112** , To appear in July issue.

Palmer T. N., Shutts G. J. and Swinbank R., 1986 : Alleviation of a systematic westerly bias in general circulation and numerical weather prediction models through an orographic gravity wave drag parametrization. *Quart. J. R. Met. Soc.* , Submitted for publication.

Pitcher E. J., Malone R. C., Ramanathan V., Blackmon M. L., Puri K. and Bourke W., 1983 : January and July simulations with a spectral general circulation model. *J. Atmos. Sci.* , **40** , 580-604.

Ramanathan V., Pitcher E. J., Malone R. C. and Blackmon M. L., 1983 : The response of a spectral general circulation model to refinements in radiative processes. *J. Atmos. Sci.* , **40** , 605-630.

Randall D. A., Abeles J. A. and Corsetti T. G., 1985 : Seasonal simulations of the planetary boundary layer and boundary-layer stratocumulus clouds with a general circulation model. *J. Atmos. Sci.*, **42**, 641-676.

Rowntree P.R., 1984 : Sensitivity of global simulations to the formulation of the evaporation of convective condensates. Workshop on convection in large–scale numerical models, 28 November–1 December 1983, ECMWF.

Slingo, A., 1985a : Simulation of the earth's radiation budget with the II-layer general circulation model. *Meteorol. Mag.*, **114**, 121-141.

Slingo, A. (Ed.), 1985b : Handbook of the Meteorological Office II-Layer Atmospheric General Circulation Model. Volume I: Model Description. Dynamical Climatology Technical Note 29. Available on request from the Dynamical Climatology Branch, Meteorological Office, London Road, Bracknell RG12 2SZ , Berkshire.

Slingo A. and Wilderspin R. C. , 1984 : Development of an improved GCM radiation scheme. IRS'84 : Current problems in atmospheric radiation . Ed. G. Fiocco . A. Deepak Publishing, Hampton, Virginia, USA.

Slingo A. and Wilderspin R. C. , 1986 : Development of a revised longwave radiation scheme for an atmospheric general circulation model. *Quart. J. R. Met. Soc.* , **112** , ~~To appear in April issue.~~ 371-386.

Slingo A. and Wilson H. , 1986 : Simulation of European climate with an atmospheric general circulation model. Current Issues In Climate Research. Ed. A. Ghazi and R. Fantechi . D. Reidel Publishing Company.

Slingo J. M., 1982 : A study of the earth's radiation budget using a general circulation model. *Quart. J. R. Met. Soc.*, **108**, 379-405.

Wallace J. M., Tibaldi S. and Simmons A. J. , 1983 : Reduction of systematic forecast errors in the ECMWF model through the introduction of an envelope orography. *Quart. J. R. Met. Soc.* , **109** , 683-717.

Wu J. , 1982 : Wind stress coefficients over sea surface from breeze to hurricane. *J. Geophys. Res.* , **87** , 9704-9706.

TABLE 1. SPECIFICATION OF CONTROL VERSION OF 11-LAYER A.G.C.M.

| ASPECT | BRIEF DESCRIPTION | REFERENCE |
|---|---|---|
| General | Global, primitive equation, sigma coordinate model | Slingo (1985b) |
| Grid | Horizontal: 2.5 x 3.75 degree latitude/longitude<br>Vertical: 11 Layers of variable thickness. | Slingo (1985a), Figure 1 |
| Basic variables | $p_*$ (surface pressure) and 11 x (u,v,T,q) | |
| Numerical Schemes | Spatial: Second order, energy conserving finite difference<br>Temporal: Explicit with 10 minute leapfrog timestep<br>Time-meaning coefficient $\alpha$ = 0.01 | As 5-Layer Model (Corby et al 1977)<br>Ditto<br>Ditto |
| Stability Filters | Computational: East-West multipoint filtering near poles<br>Noise: Non-linear horizontal diffusion. | -<br>Developed from 5-Layer Model. |
| Topography | Realistic land-sea mask. Mean orography. | Gates and Nelson (1973) |
| Dynamics | Flux form of equations used. Includes virtual temperature effects. | Similar to 5-Layer Model |
| SST's/Sea-Ice | Prescribed from climatology. Updated every 5 days. | As 5-Layer Model (J M Slingo 1982) |
| Land Surface | Interactive surface temperature, soil moisture content and snow depth. | Carson (1982a) |
| Surface exchanges | Stability-dependent exchange coefficients.<br>Evaporation limited by soil moisture content and by surface resistance $r_s$ = 60 $sm^{-1}$. | Carson (1982a)<br>-<br>- |
| Ekman fluxes | Eddy diffusivity approach in lowest three layers | Carson (1982b) |
| Large-scale precipitation | Forms at 100% relative humidity. Includes ice-phase (snow). | Similar to 5-Layer Model. |
| Convection | Penetrative convection scheme. Includes ice phase (snow). | Rowntree (1984) |
| Radiation/Clouds | Interactive scheme. Prescribed cloudiness. Realistic surface albedos. Fractional cloud cover treated. Called every 3 hours to resolve diurnal cycle. | Slingo (1985a), revised by Slingo and Wilderspin (1984/1986) |

## FIGURE CAPTIONS

Figure 1 Pressure at mean sea level (PMSL) in millibars (mb) for the northern winter season (December to February) for the mean of (a) the 3 winters 1983/1984 to 1985/1986 derived from Meteorological Office operational analyses and (b) 8 winters from the control experiment. The contour interval is 8 mb.

Figure 2 Pressure at mean sea level (PMSL) in millibars (mb) for the northern summer season (June to August) for the mean of (a) the 3 summers 1983 to 1985 derived from Meteorological Office operational analyses and (b) 8 summers from the control experiment. The contour interval is 8 mb.

Figure 3 As Figure 1 but for 500 mb geopotential height in decametres (dam). The contour interval is 12 dam.

Figure 4 As Figure 1 but for 250 mb winds ($ms^{-1}$) and isotachs ( contours at 10, 20, and every 20 $ms^{-1}$ thereafter).

Figure 5 As Figure 1 but for zonally-averaged zonal winds ($ms^{-1}$) and temperatures (K) as a function of pressure.

Figure 6 As Figure 2 but for zonally-averaged zonal winds ($ms^{-1}$) and temperatures (K) as a function of pressure.

Figure 7 Total precipitation (rain plus snow) for the northern winter season for (a) the data of Jaeger (1983) and (b) 8 winters from the control experiment. The contours are at 0.1, 1, 2, 5 and 10 mm/day with shading above 5 mm/day.

Figure 8 Pressure at mean sea level (PMSL) in millibars (mb) for the northern winter season (December to February) for the mean of 4 winters from (a) the truncated envelope orography experiment and (b) the experiment with the gravity wave drag scheme. The contour interval is 8 mb. Compare with Figure 1.

Figure 9 As Figure 8 but for 500 mb geopotential height in decametres (dam). The contour interval is 12 dam. Compare with Figure 3.

Figure 10 As Figure 8 but for 250 mb winds ($ms^{-1}$) and isotachs (contours at 10, 20 and every 20 $ms^{-1}$ thereafter). Compare with Figure 4.

Figure 11 As Figure 8 but for zonally-averaged zonal winds ($ms^{-1}$) and temperatures (K) as a function of pressure. Compare with Figure 5.

Figure 12 As Figure 8 but for total precipitation (rain plus snow). Compare with Figure 7.

Figure 13 Pressure at mean sea level (PMSL) in millibars (mb) for the northern summer season (June to August) for the mean of 3 summers from (a) the truncated envelope orography experiment and (b) the experiment with the gravity wave drag scheme. The contour interval is 8 mb. Compare with Figure 2.

Figure 14 As Figure 13 but for zonally-averaged zonal winds ($ms^{-1}$) and temperatures (K) as a function of pressure. Compare with Figure 6.

Figure 15 Northern hemisphere polar stereographic maps of the standard deviation of the high-pass filtered daily 500 mb heights ( in dam ) for the northern winter season from (a) Meteorological Office analyses for the 3 winters 1983/1984 to 1985/1986, (b) 8 winters from the control experiment, (c) 4 winters from the truncated envelope orography experiment and (d) 4 winters from the experiment with the gravity wave drag scheme. See section 5 for an explanation of how the data were processed.

a) Observed

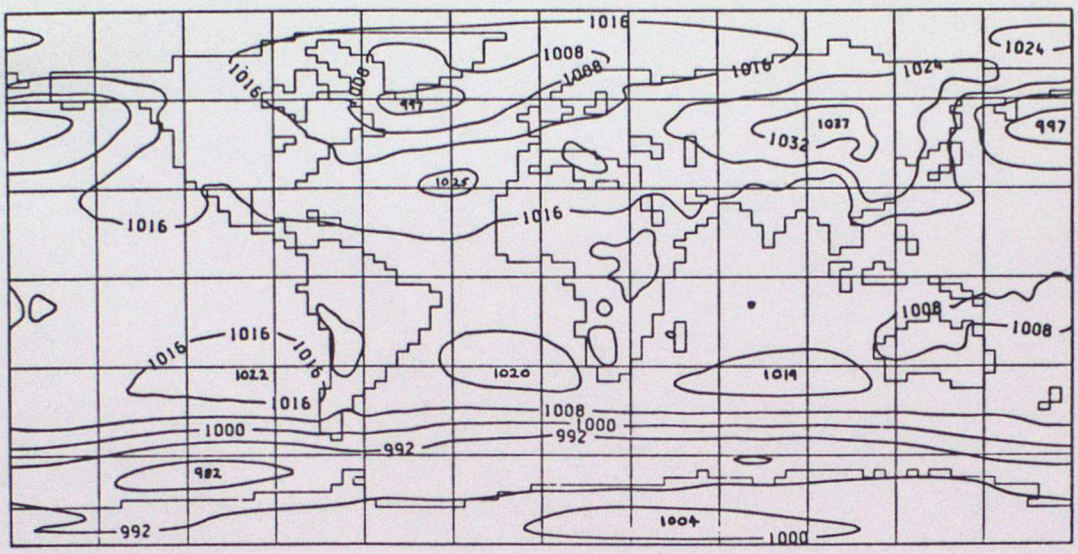


b) Control

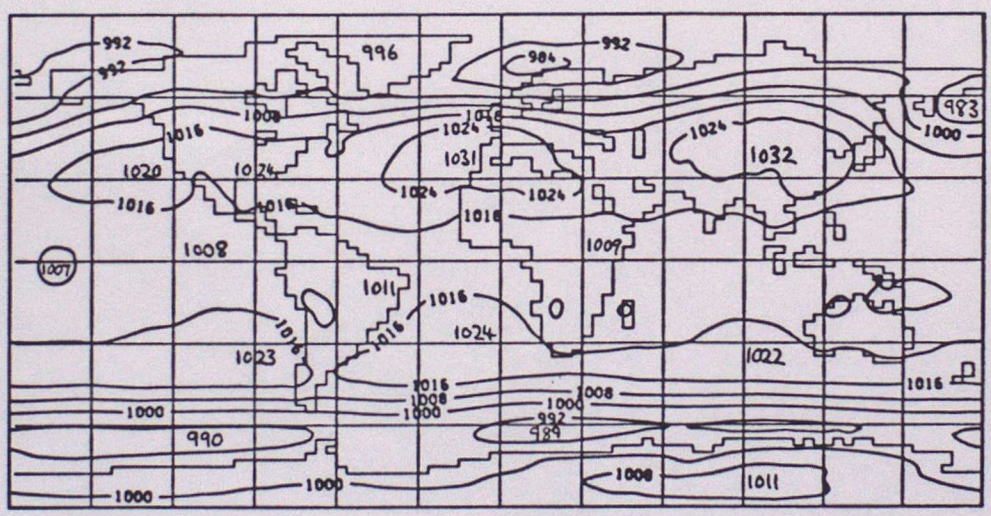


Fig. 1

a) Observed

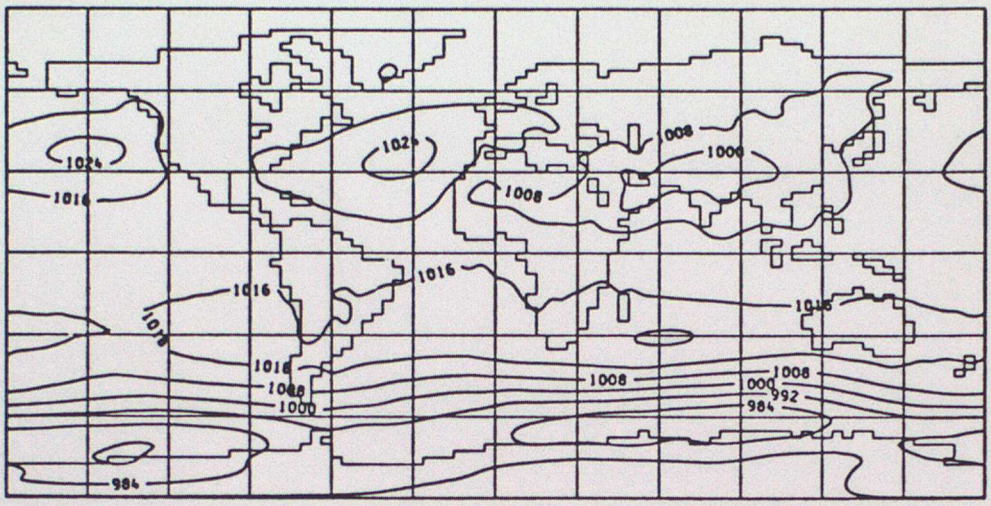


b) Control

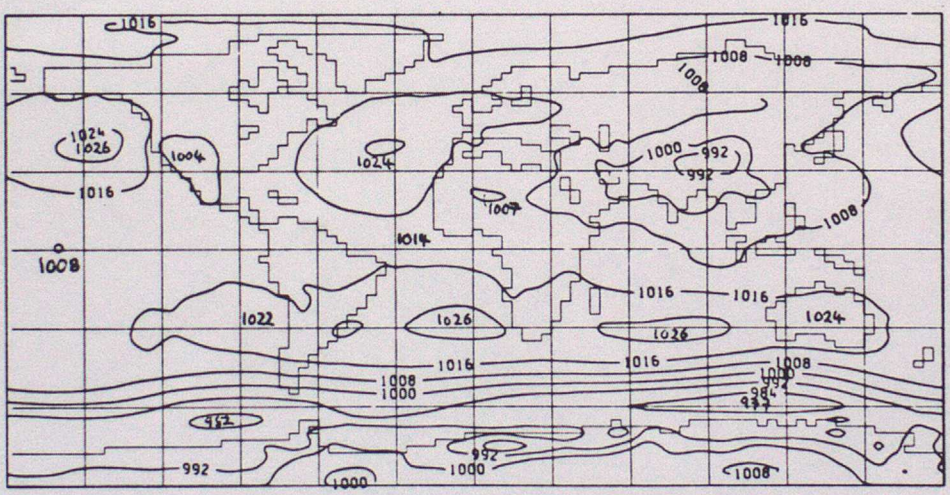


Fig. 2

a) Observed

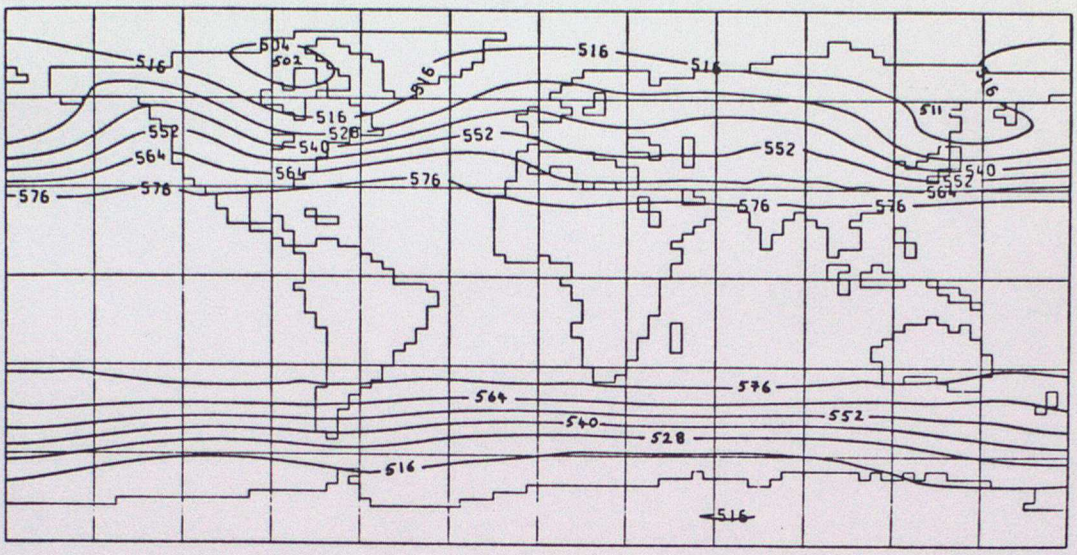


b) Control

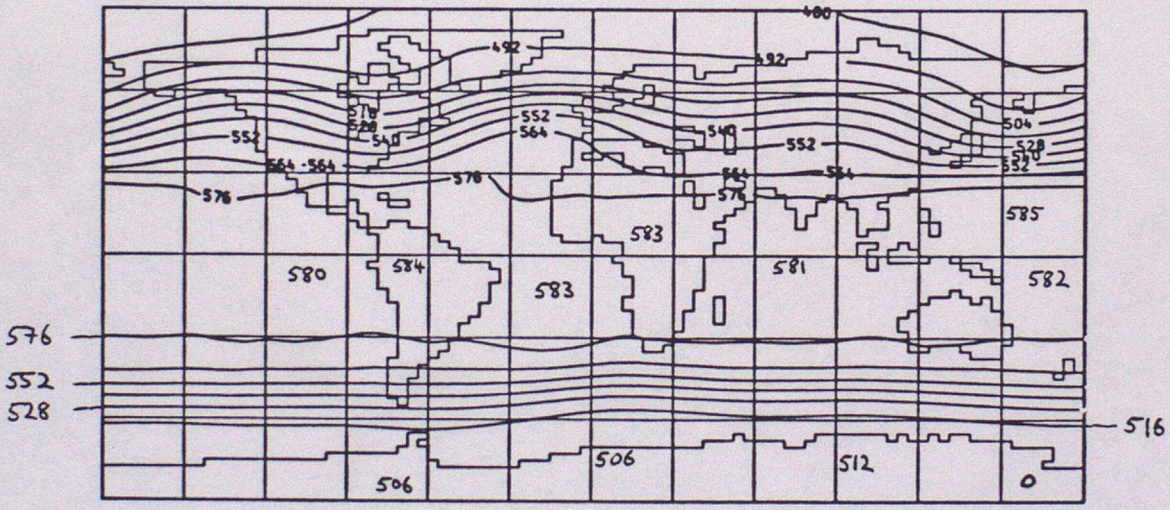


Fig. 3

a) Observed

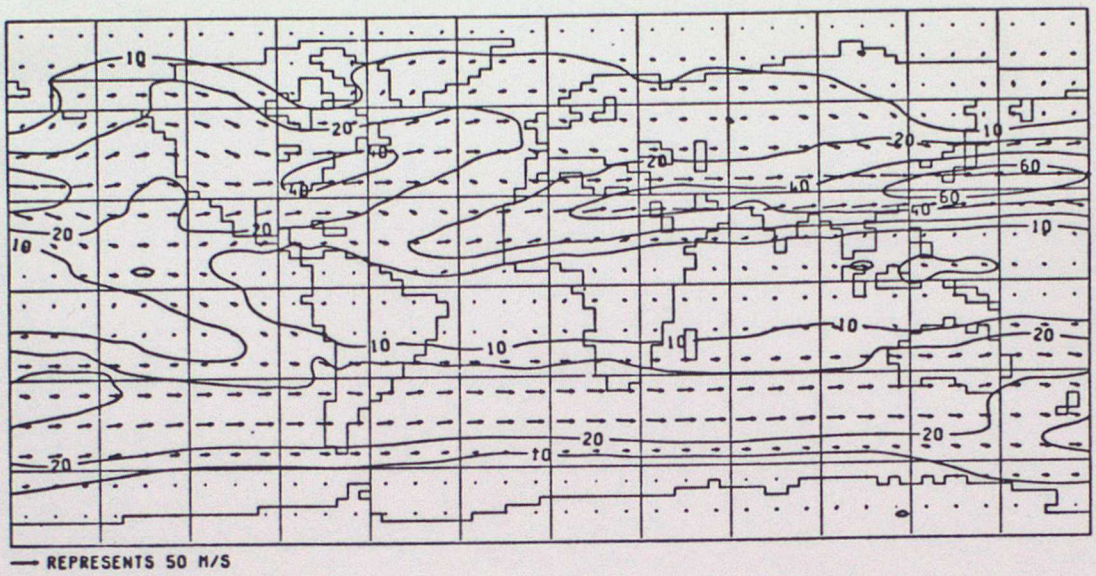


b) Control

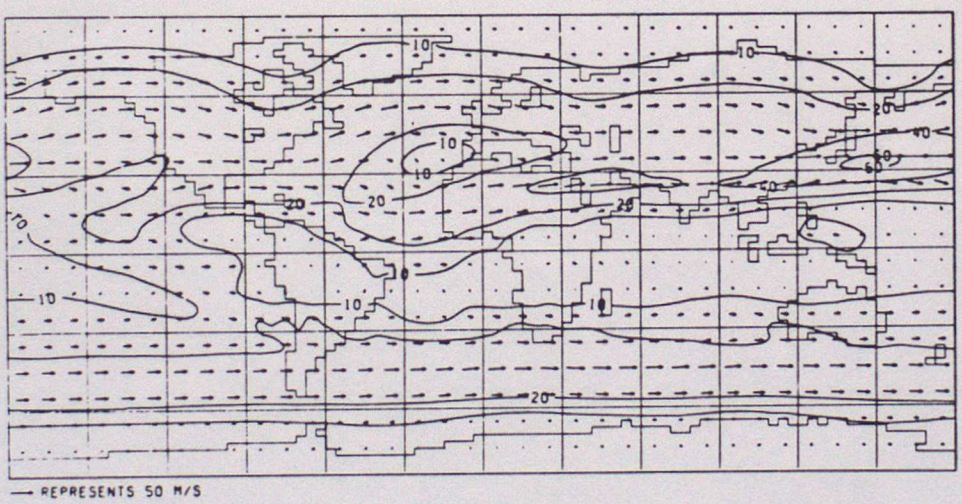


Fig. 4

a) Observed

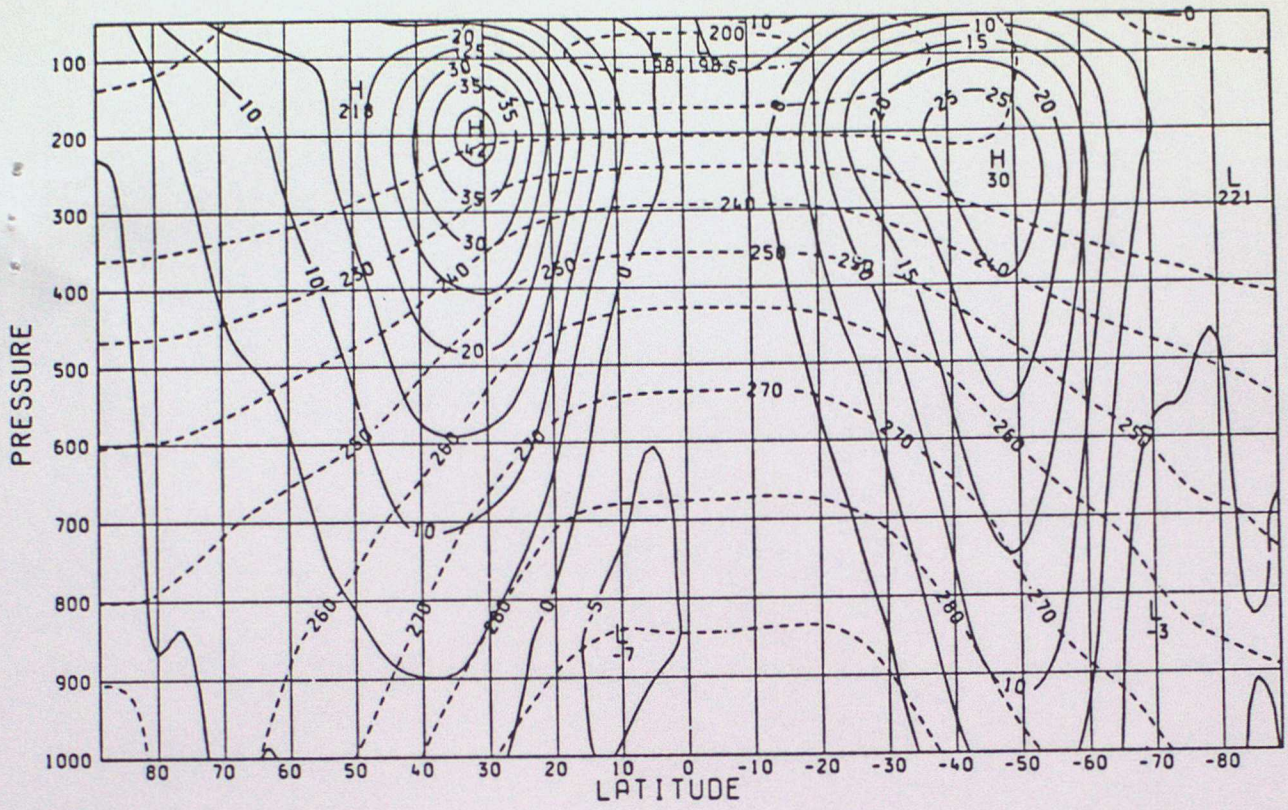


b) Control

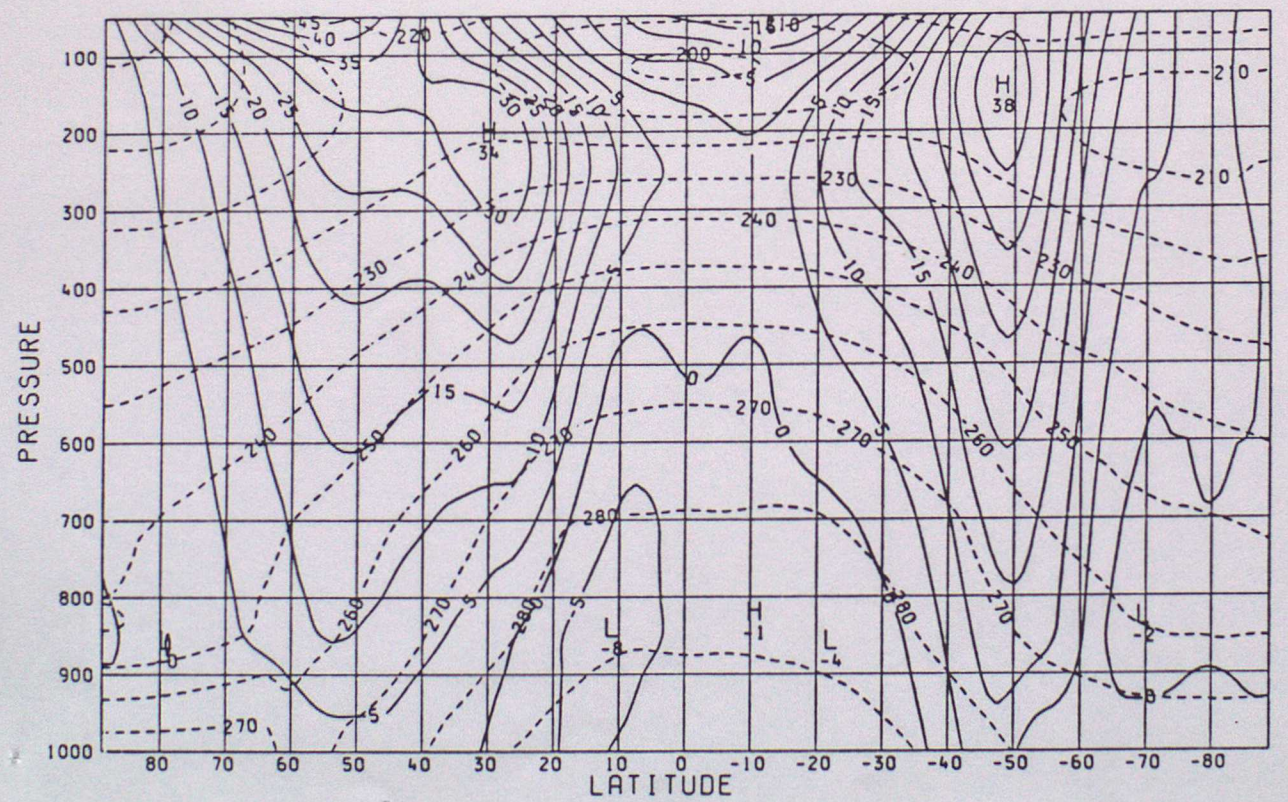


Fig. 5

a) Observed

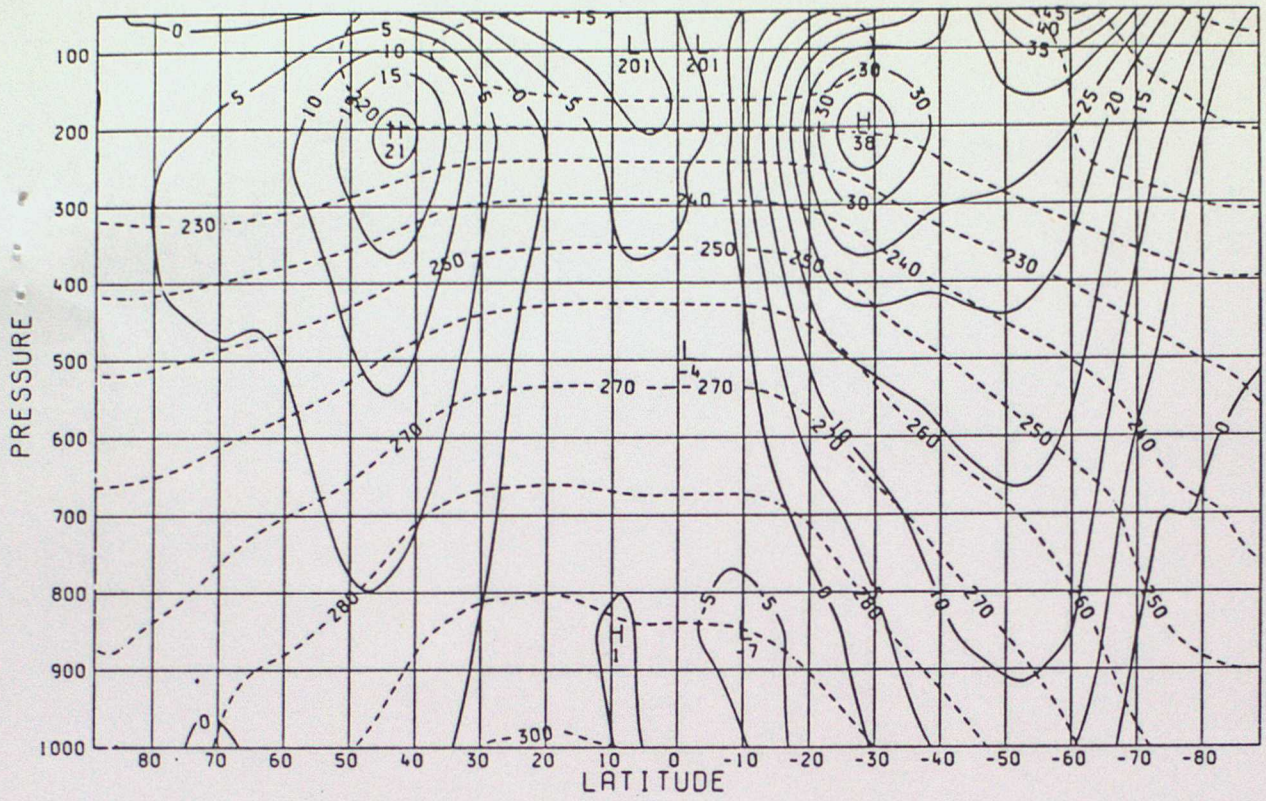


b) Control

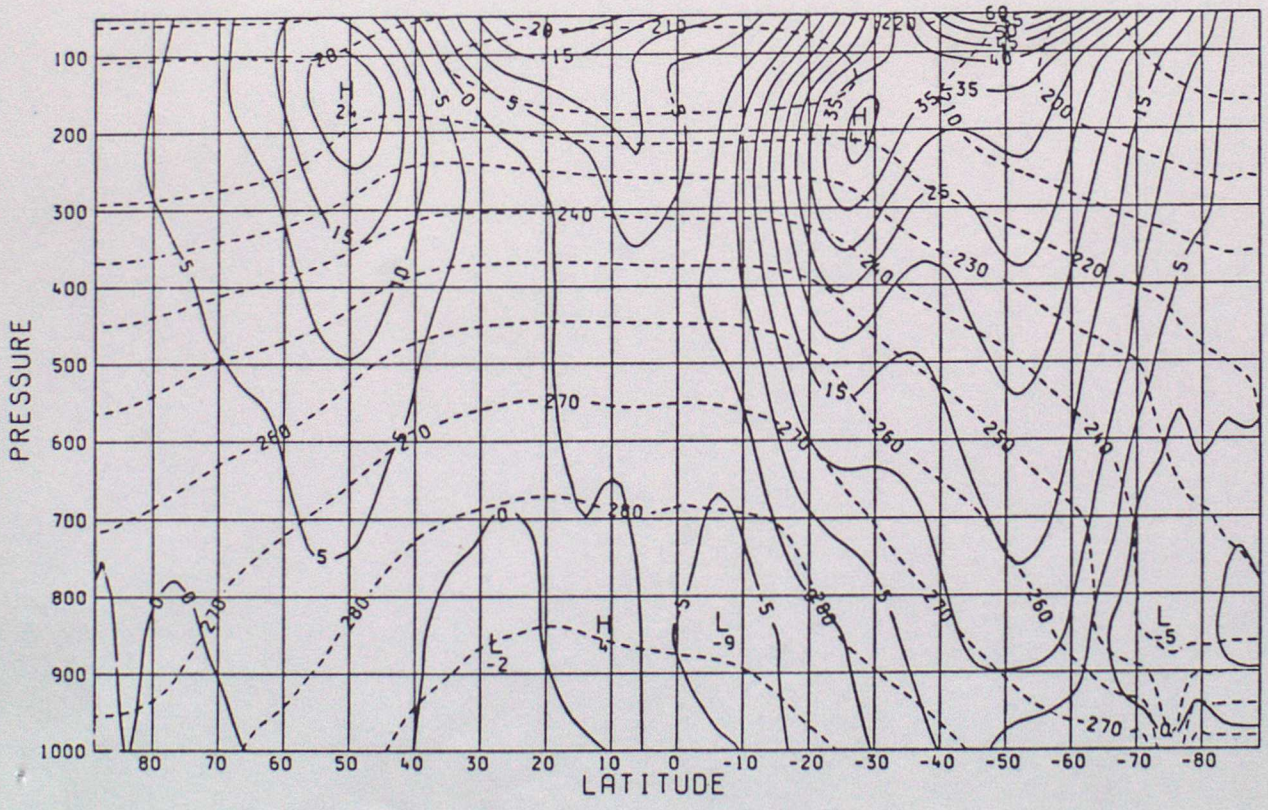


Fig. 6

a) Observed

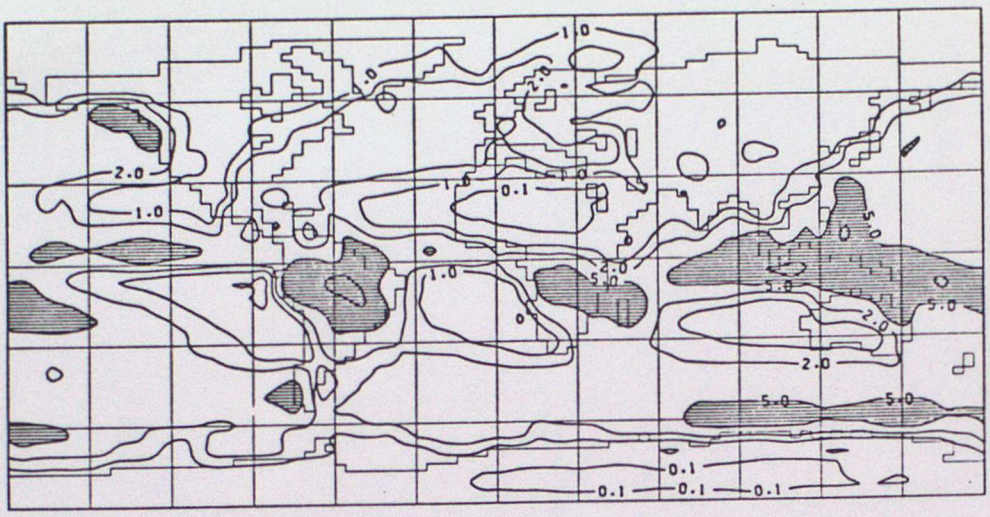


b) Control

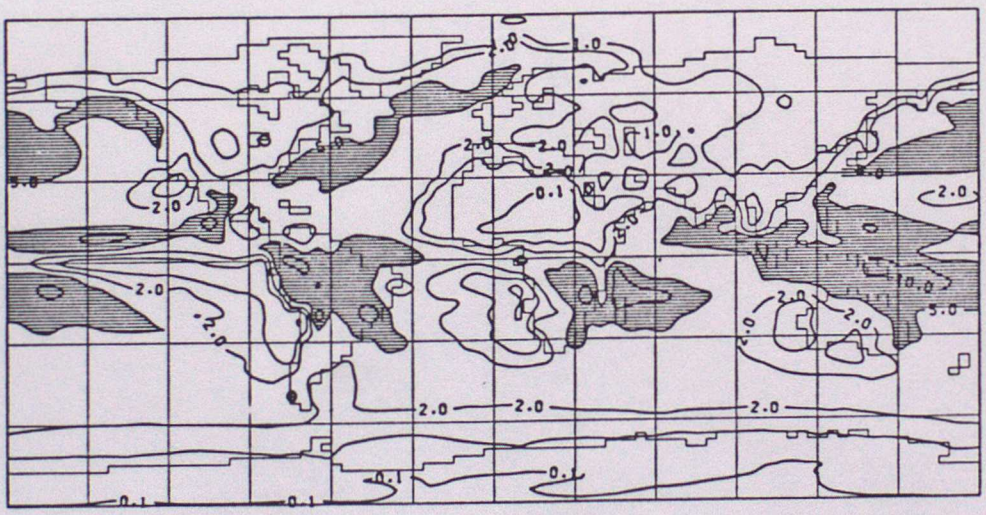


Fig. 7

a) Tenv

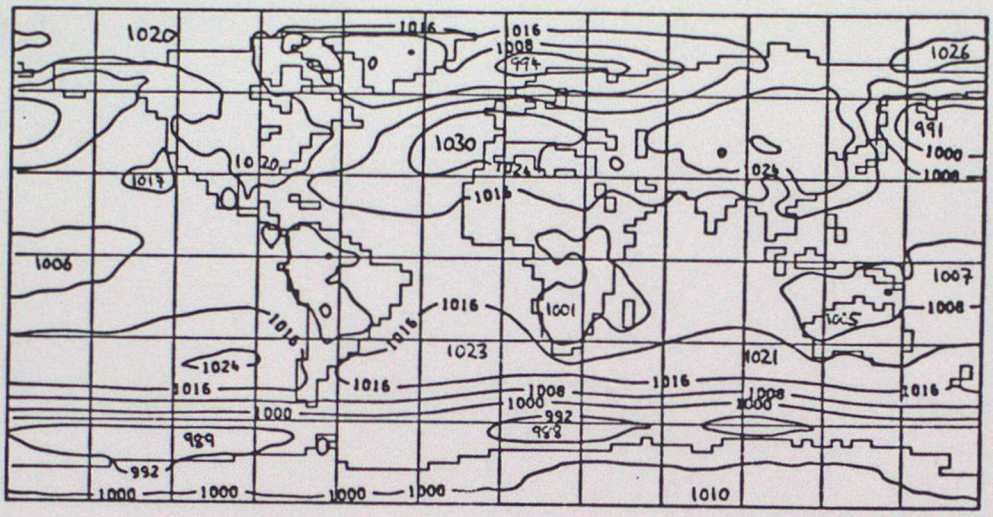


b) Grav

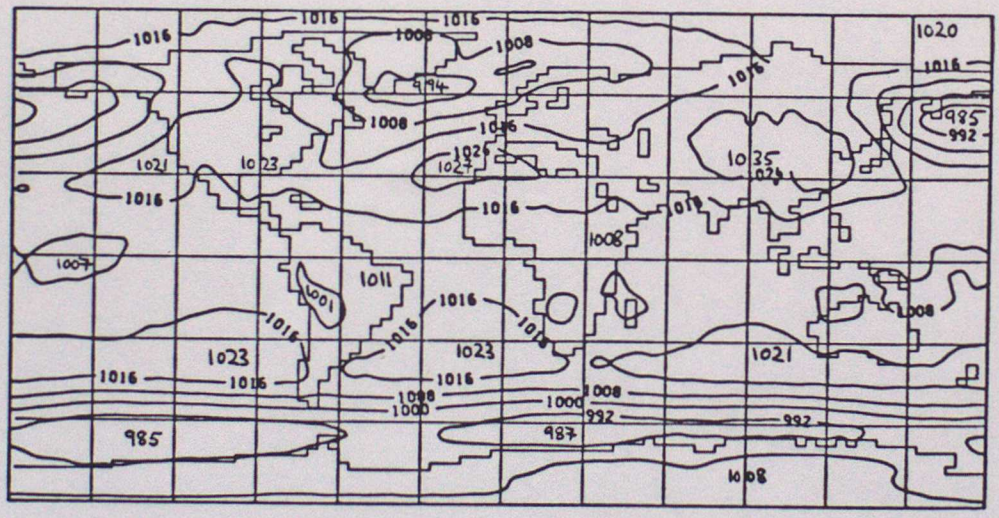


Fig. 8

a) Tenv

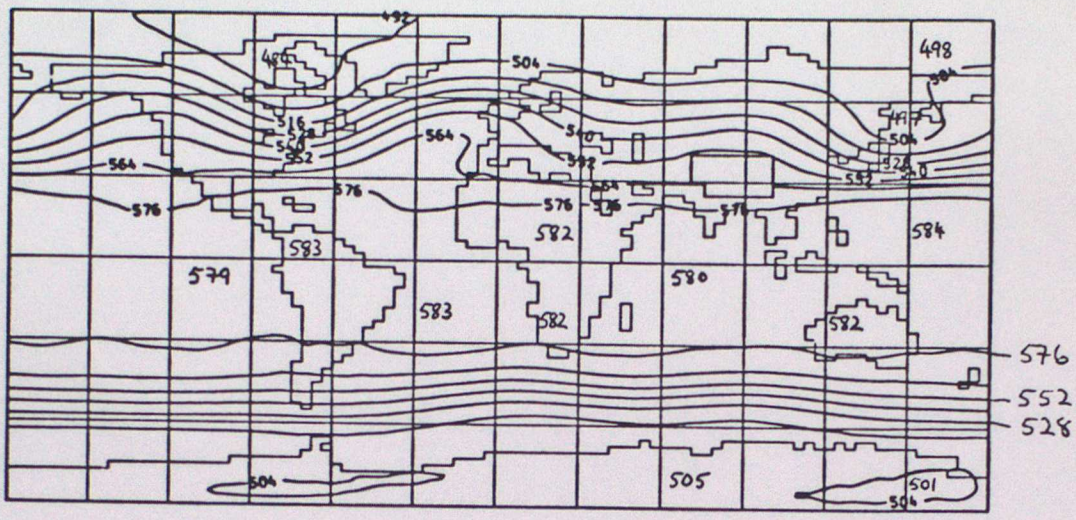


b) Grav

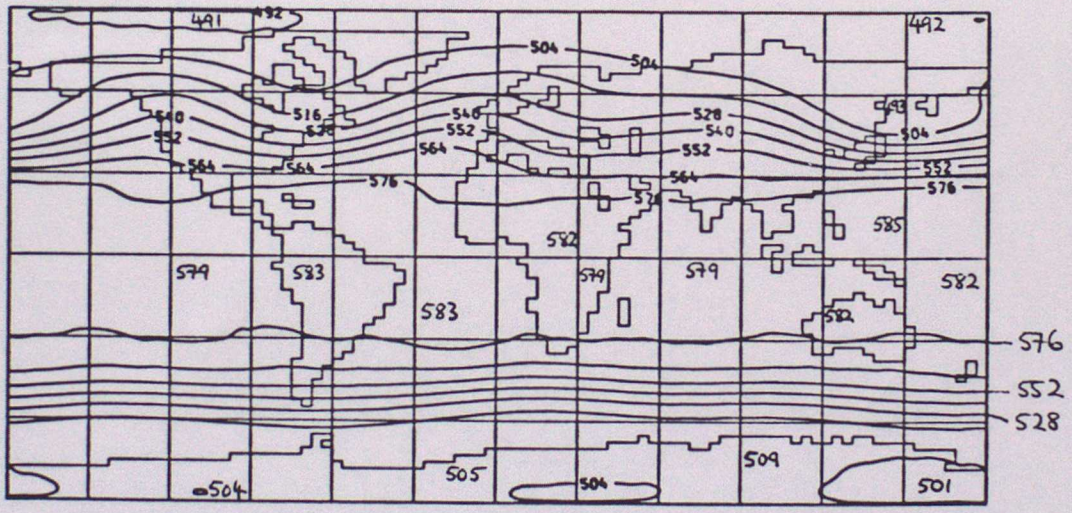


Fig. 9

a) Tenv

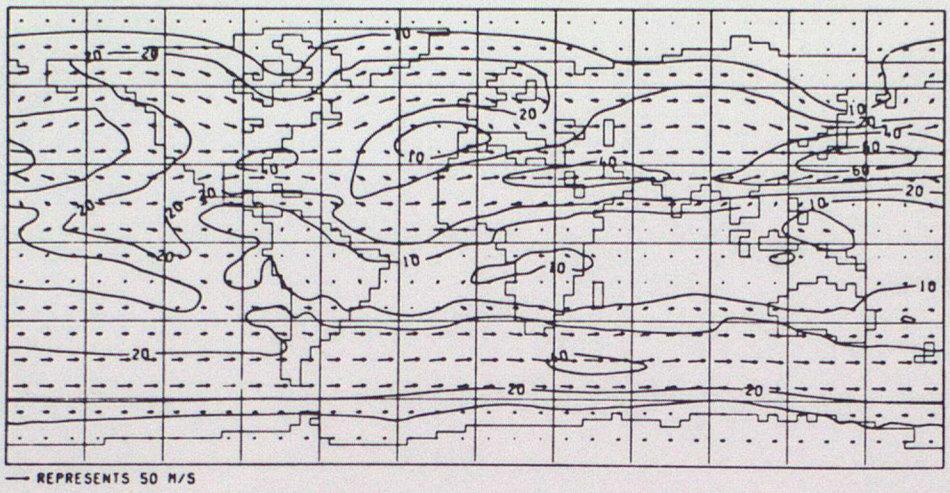


b) Grav

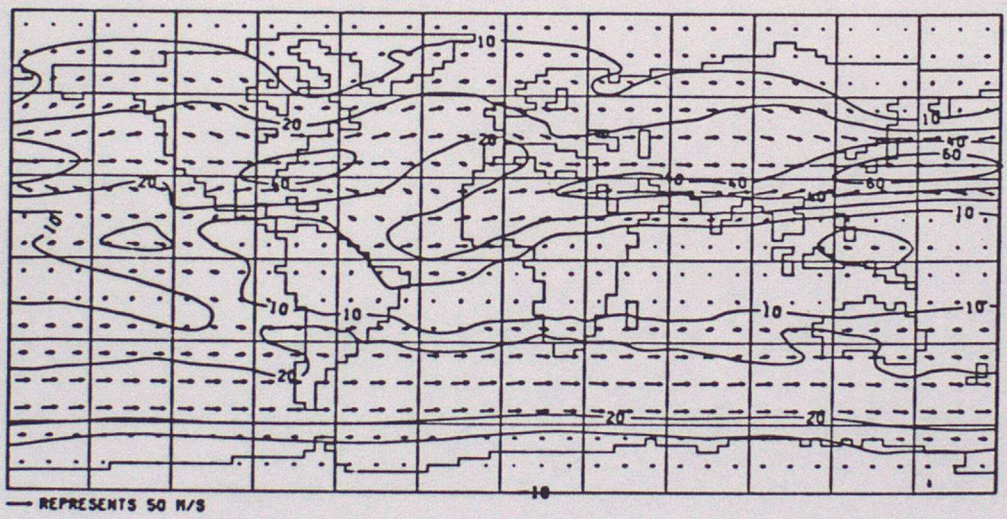


Fig. 10

a) Tenv

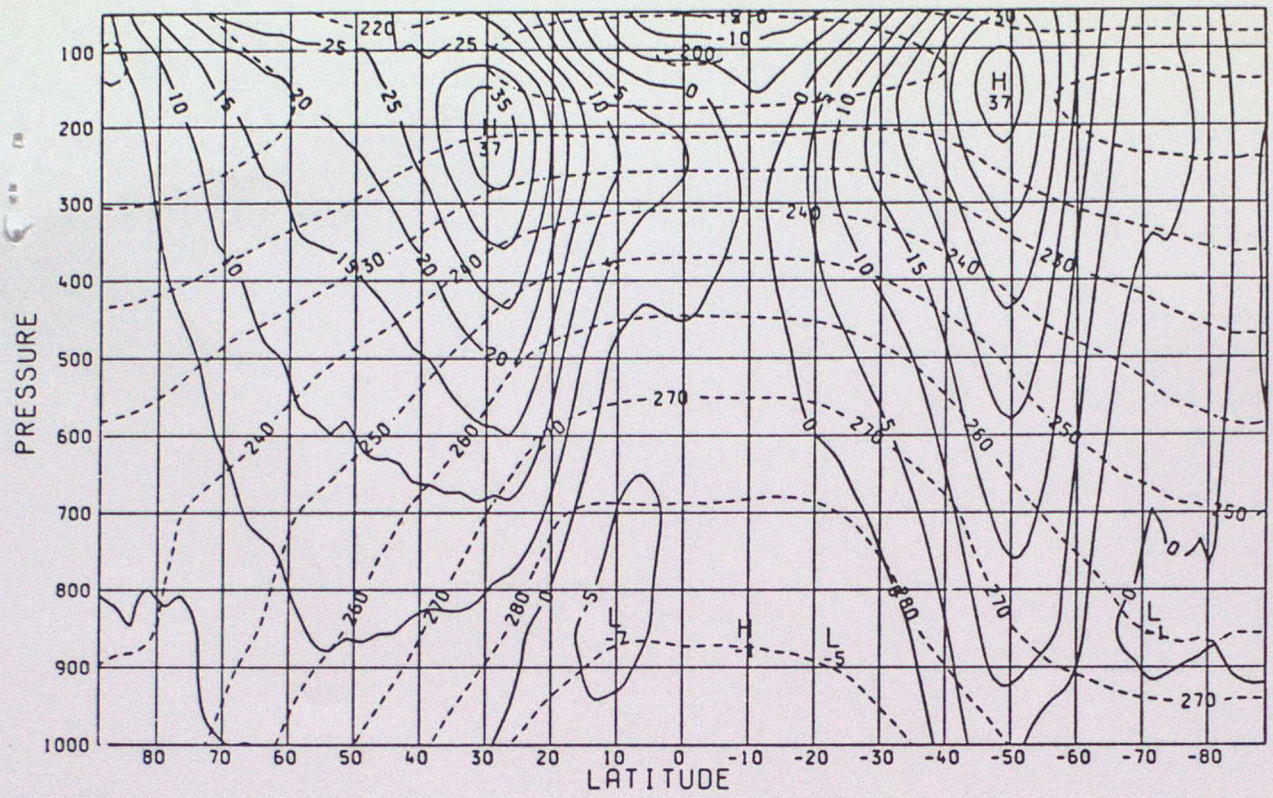


b) Grav

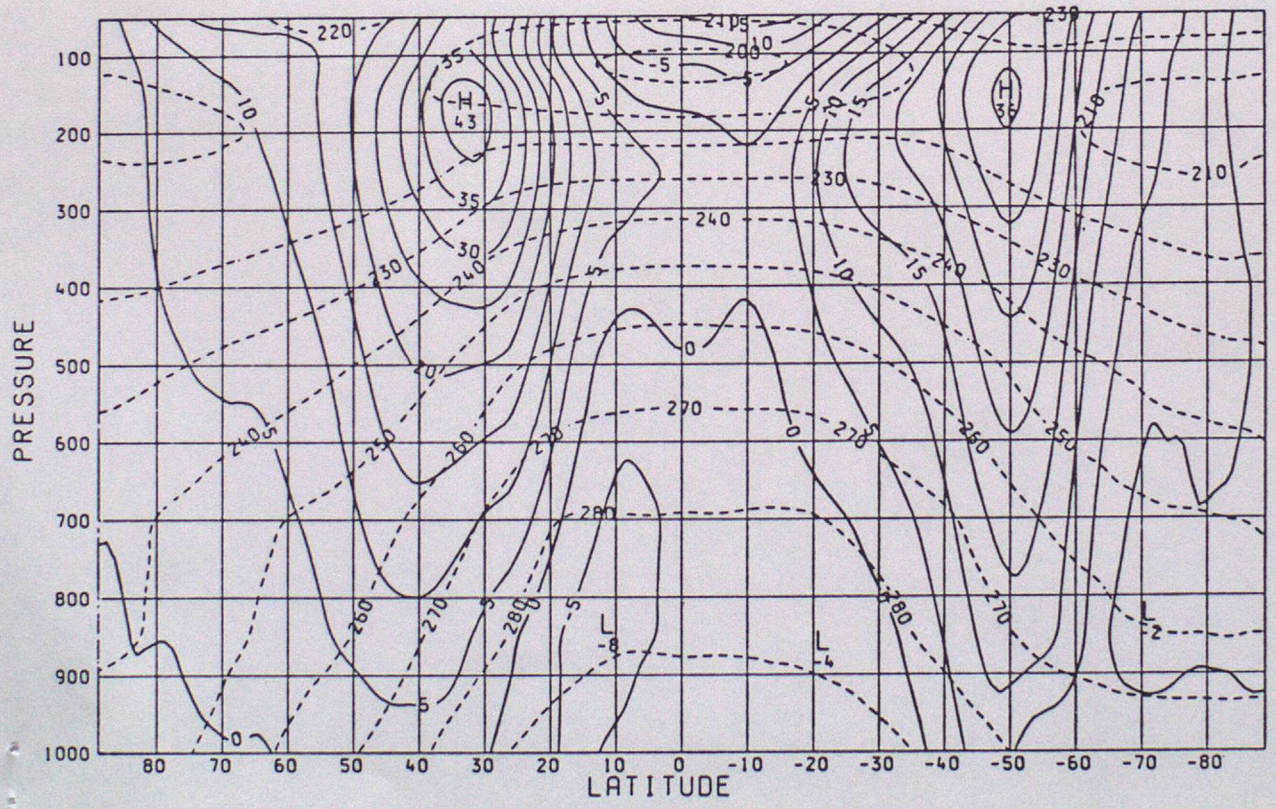


Fig. 11

a) Tenv

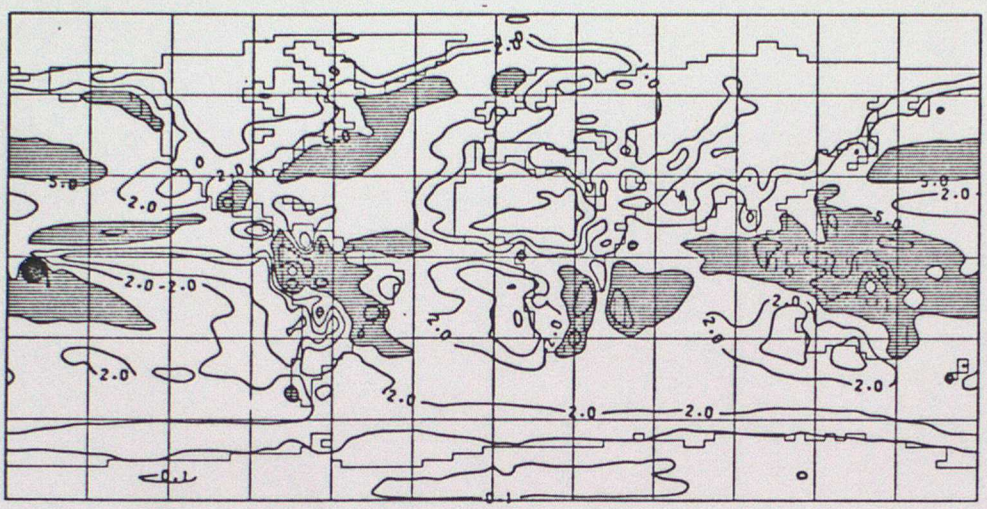


b) Grav

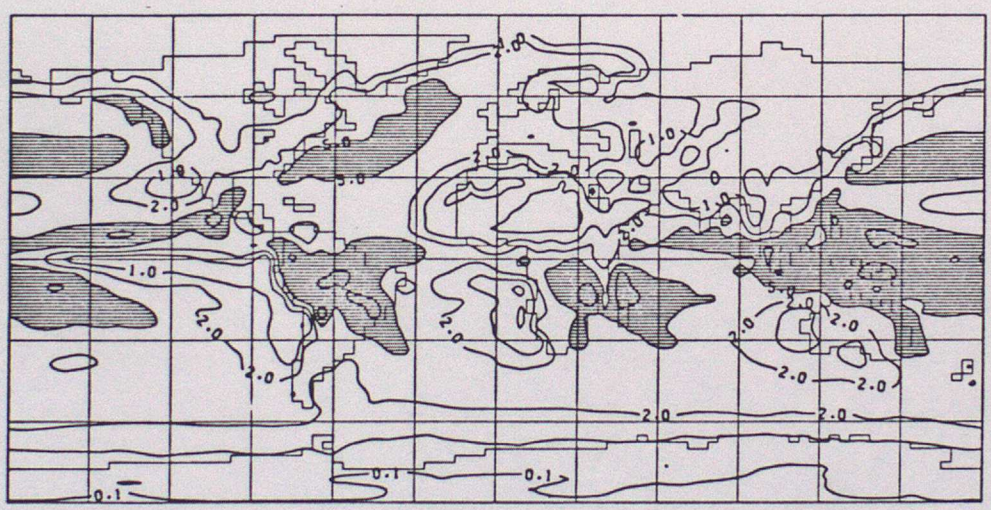


Fig. 12

a) Tenv

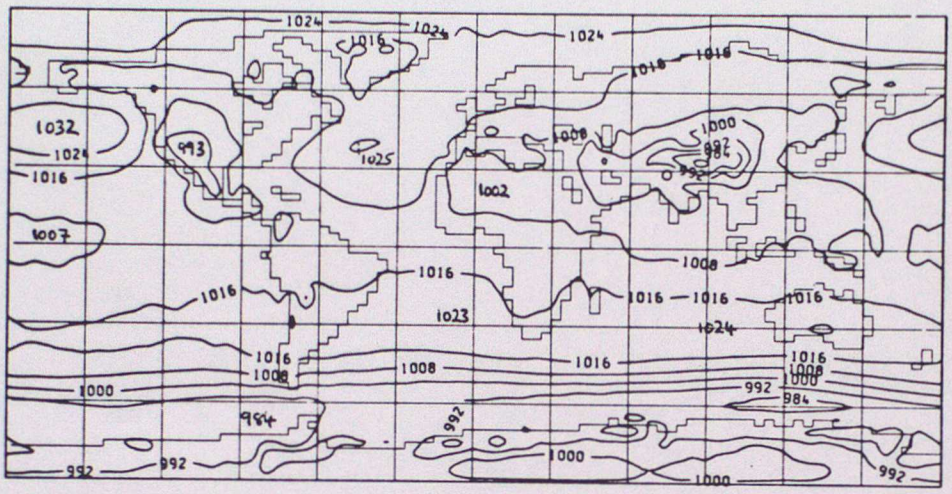


b) Grav

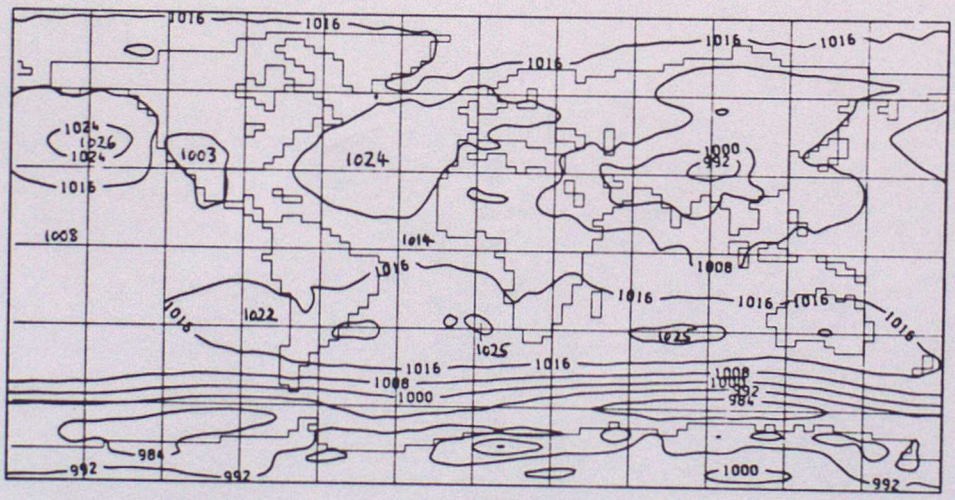


Fig. 13

a) Tenv

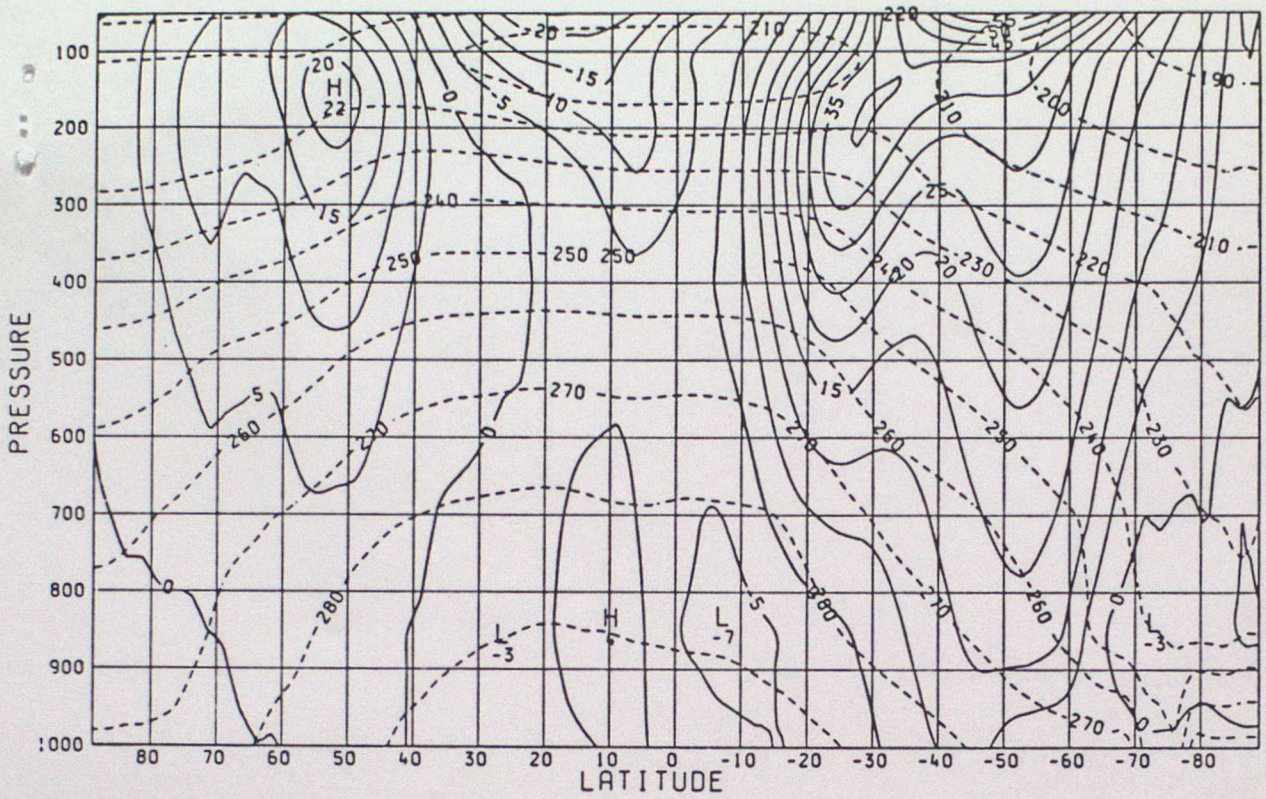


b) Grav

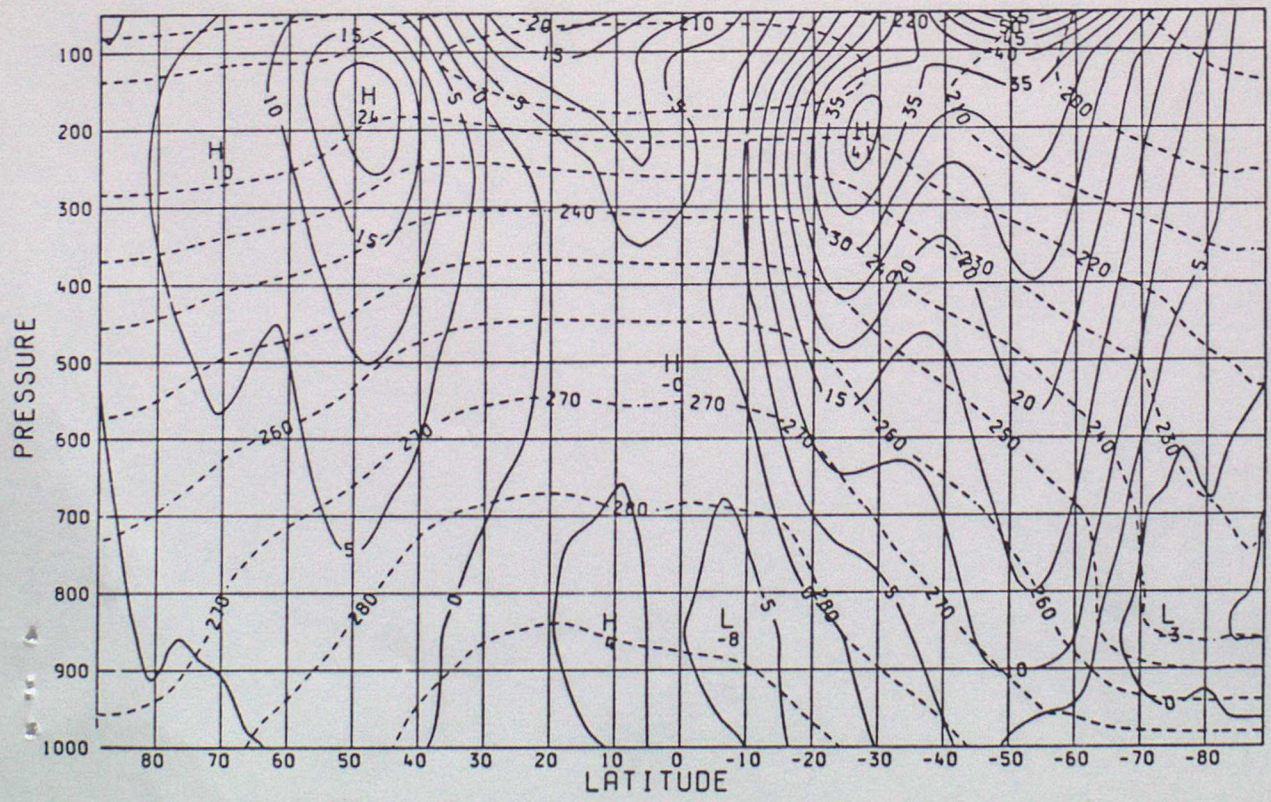


Fig. 14

a) OBSERVED

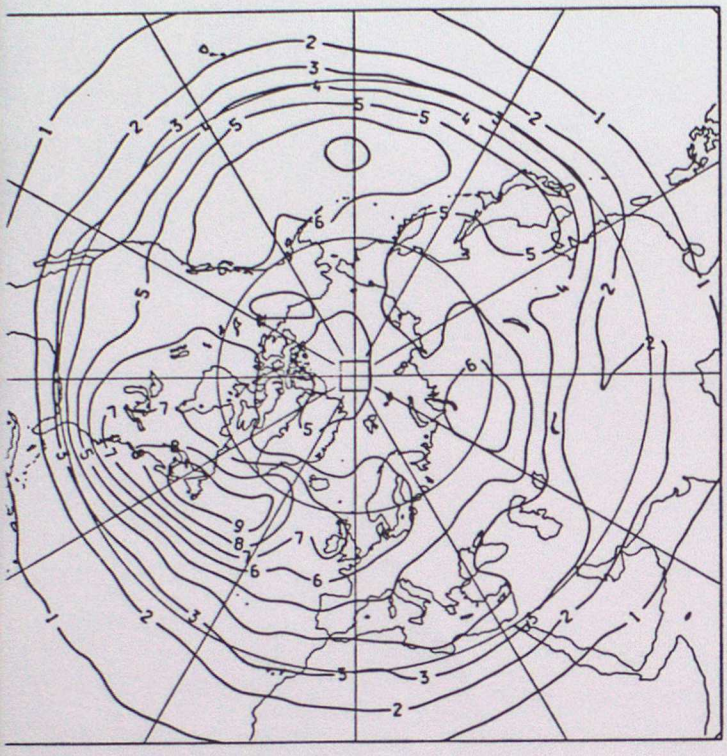

c) TENV

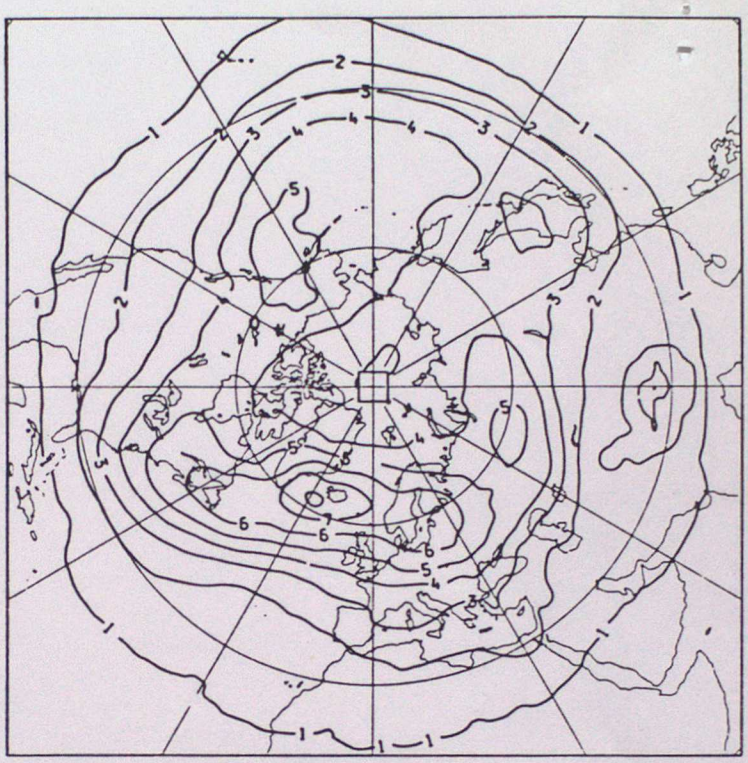

b) CONTROL

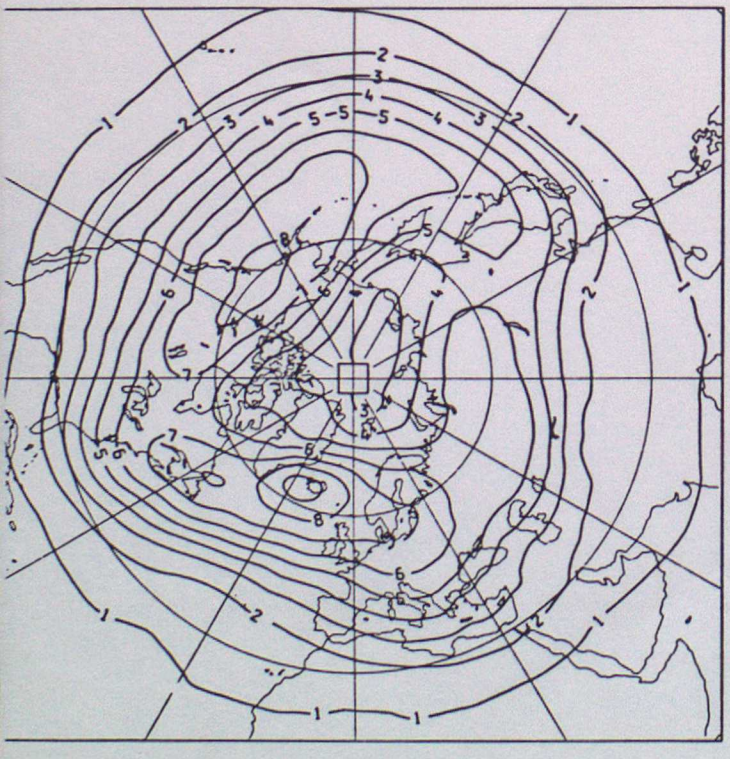

d) GRAV

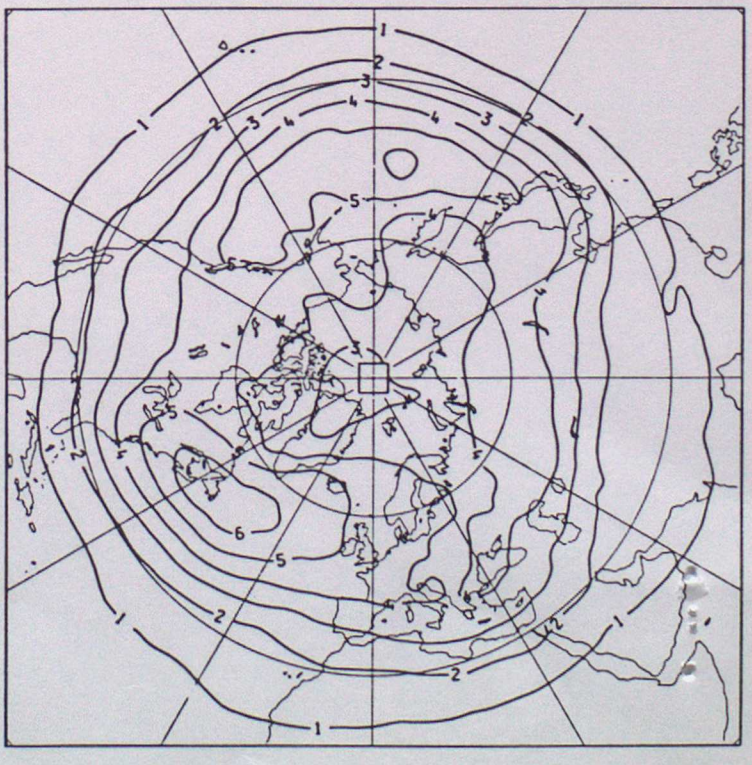

Fig. 15

DYNAMICAL CLIMATOLOGY TECHNICAL NOTES

| | | |
|---|---|---|
| DCTN 1 | June 1984 | A scheme for incorporating the thermodynamic sea-ice model into a coupled ocean-atmosphere model.<br>C Gordon and M Bottomley |
| DCTN 2 | Sept 1984 | The parametrization of the upper ocean mixed layer in coupled ocean/atmosphere models.<br>C Gordon and M Bottomley |
| DCTN 3 | Sept 1984 | The response of a simple thermodynamic sea-ice model to GCM forcing appropriate for perennial sea-ice.<br>M Bottomley |
| DCTN 4 | Sept 1984 | Potential vorticity in the stratosphere derived using data from satellites.<br>S A Clough, N S Grahame and A O'Neill |
| DCTN 5 | Sept 1984 | Simulation of the seasonal cycle of SST using globally specified climatological data to force simple ocean models.<br>N S Grahame |
| DCTN 6 | Sept 1984 | Development of an improved GCM radiation scheme.<br>A Slingo and R C Wilderspin |
| DCTN 7 | Sept 1984 | On the specification of surface fluxes in coupled atmosphere/ocean general circulation models.<br>J F B Mitchell, C A Wilson and C M Price |
| DCTN 8 | Sept 1984 | A survey of possible repercussions of the Soviet river reversal programme on Arctic sea-ice.<br>H Cattle |
| DCTN 9 | Oct 1984 | A study of a strong stratospheric warming during January 1982<br>T D A Fairlie |
| DCTN 10 | Nov 1984 | An intercomparison of the Met O 11 N45 model and the Met O 20 11-level model on the Cyber 205<br>J F Dyson |
| DCTN 11 | Nov 1984 | Simulation of observed time series of temperature and precipitation over eastern England.<br>D N Reed |
| DCTN 12 | Nov 1984 | Forecasts and analyses of the onset of the Southwest monsoon.<br>R Kershaw |
| DCTN 13 | Nov 1984 | On modelling the effects of $CO_2$ on climate.<br>J F B Mitchell |
| DCTN 14 | Dec 1984 | Development of a revised longwave radiation scheme for an atmospheric general circulation model.<br>A Slingo and R C Wilderspin |
| DCTN 15 | Jan 1985 | Rossby wavetrains in the stratosphere forced by localised disturbances in the troposphere.<br>C J Marks (Oxford), A O'Neill and V D Pope |

DYNAMICAL CLIMATOLOGY TECHNICAL NOTES

| | | |
|---|---|---|
| DCTN 16 | Jan 1985 | Observing system experiments using the Meteorological Office's 15-level model.<br>R A Bromley |
| DCTN 17 | Feb 1985 | Atmospheric general circulation simulation of the climate of the Mediterranean region.<br>H Cattle |
| DCTN 18 | Feb 1985 | Diurnal variation and cloud in a general circulation model.<br>C A Wilson and J F B Mitchell |
| DCTN 19 | Feb 1985 | The sensitivity of the Saharan region in a general circulation model.<br>W M Cunnington and P R Rowntree |
| DCTN 20 | Mar 1985 | The impact of aircraft observations on analyses and forecasts from the operational 15-level model.<br>B R Barwell |
| DCTN 21 | Mar 1985 | Non-linear effects on heat-induced circulation of the tropical atmosphere.<br>A E Gill and P J Phlips |
| DCTN 22 | Apr 1985 | Simulation of cloudiness with the U.K. Meteorological Office 11-layer AGCM.<br>A Slingo and R C Wilderspin |
| DCTN 23 | Apr 1985 | An integrated approach to the representation of cloud processes. R N B Smith |
| DCTN 24 | May 1985 | Nuclear Winter: Calculations of the shortwave radiative effects of soot aerosols.<br>A Slingo and P Goldsmith |
| DCTN 25 | Jul 1985 | Sea ice and the Antarctic winter circulation: a numerical experiment.<br>J F B Mitchell and T S Hills |
| DCTN 26 | Jul 1985 | A Budyko-Sellers model for study of ocean-atmosphere interaction.<br>W J Ingram |
| DCTN 27 | Aug 1985 | The effect of a shoaling thermocline on equatorially-trapped Kelvin waves.<br>A E Gill and B A King |
| DCTN 28 | Sept 1985 | $CO_2$ climate sensitivity and model dependence of results.<br>J F B Mitchell, C A Wilson and W M Cunnington |
| DCTN 29 | Sept 1985 | Handbook of the Meteorological Office 11-layer atmospheric general circulation model.<br>Volume 1 : Model Description<br>Edited by A Slingo |
| DCTN 30 | Sept 1985 | Impact of land surface variations on African rainfall in general circulation models.<br>P R Rowntree, M F Wilson and A B Sangster |

DYNAMICAL CLIMATOLOGY TECHNICAL NOTES

| | | |
|---|---|---|
| DCTN 31 | Nov 1985 | The annual cycle of sea level in the eastern tropical Pacific.<br>G R Bigg and A E Gill |
| DCTN 32 | Nov 1985 | An analytic model of the heat-induced tropical circulation in the presence of a mean wind.<br>P J Phlips and A E Gill |
| DCTN 33 | Nov 1985 | The effect of resolution and diffusion on the simulated climate.<br>J F Dyson |
| DCTN 34 | Jan 1986 | Rossby adjustment over a step.<br>M K Davey, A E Gill, E R Johnson and P F Linden |
| DCTN 35 | Jan 1986 | Issues concerning the evaluation of effective surface roughness of heterogeneous terrain.<br>D J Carson |
| DCTN 36 | Mar 1986 | Climate sensitivity and past climates : evidence from numerical studies<br>J F B Mitchell |
| DCTN 37 | Mar 1986 | Parametrizations of land-surface processes in Meteorological Office numerical weather prediction and climate models<br>D J Carson |
| DCTN 38 | Apr 1986 | Modelling of land-surface processes and their influence on European Climate<br>D A Warrilow, A B Sangster and A Slingo |
| DCTN 39 | Apr 1986 | Simulation of climatic change due to increased $CO_2$<br>J F B Mitchell |
| DCTN 40 | May 1986 | On the interpretation of the Eliassen-Palm flux divergence.<br>Part I : Theory<br>D G Andrews |
| DCTN 41 | June 1986 | Experiments on tropical circulation with a simple moist model.<br>M K Davey and A E Gill |
| DCTN 42 | Jun 1986 | Parameter regimes for studying isolated eddies.<br>P D Killworth and M K Davey |